2020

Testing glacial isostatic adjustment models of last-interglacial sea level history in the Bahamas and Bermuda

Daniel R. Muhs
U.S. Geological Survey, dmuhs@usgs.gov

Kathleen R. Simmons
U.S. Geological Survey

R. Randall Schumann
U.S. Geological Survey

Eugene S. Schweig
U.S. Geological Survey

Mark P. Rowe
Shinbone Alley, St Georges, Bermuda

Testing glacial isostatic adjustment models of last-interglacial sea level history in the Bahamas and Bermuda

Daniel R. Muhs [a, *], Kathleen R. Simmons [a], R. Randall Schumann [a], Eugene S. Schweig [a], Mark P. Rowe [b]

[a] U.S. Geological Survey, MS 980, Box 25046, Federal Center, Denver, CO, 80225, USA
[b] 5 Shinbone Alley, St Georges GE05, Bermuda

ABSTRACT

Part of the spatial variation in the apparent sea-level record of the last interglacial (LIG) period is due to the diverse response of coastlines to glacial isostatic adjustment (GIA) processes, particularly where coastlines were close to the Laurentide Ice Sheet during the past two glacial periods. We tested modeled LIG paleo-sea levels on New Providence Island (NPI), Bahamas and Bermuda by investigating emergent coral patch reefs and oolitic/peloidal beach deposits. Corals with closed-system histories collected from patch reefs on NPI have ages of 128-118 ka and ooids/peloids from beach ridges have closed-system ages of 128-116 ka. Elevations of patch reefs indicate a LIG paleo-sea level of *at least* ~7 m to ~9 m above present. Beach ridge sediments indicate paleo-sea levels of ~5 m to ~14 m (assuming subsidence, ~7 m to ~16 m) above present during the LIG. Some, though not all of these measurements are in good agreement with GIA models of paleo-sea level that have been simulated for the Bahamas. On Bermuda, corals with closed-system histories collected from marine deposits have ages of 126-114 ka. Although coral-bearing marine deposits on Bermuda lack the precise indication of paleo-sea level provided by patch reefs and oolitic beach ridges, these sediments nevertheless provide at least a first-order estimate of paleo-sea level. Paleo-sea level records on Bermuda are consistently lower (~2 m to ~7 m) than what GIA models simulate for the LIG. The reason for the reasonable agreement with models for the Bahamas and poor agreement for Bermuda is not understood, but needs further investigation in light of the probability of a higher sea level in the near future.

Published by Elsevier Ltd.

1. Introduction

With the prospect of a substantially higher sea level by the end of the current century, under almost any future climate warming scenario (Church et al., 2013), there has been an increased interest in understanding the causes and magnitudes of past high sea levels. One such period that has been studied for this purpose is the peak of the last interglacial (LIG) complex, equivalent to marine isotope stage (MIS) 5.5 or 5e (Martinson et al., 1987). This relatively high sea stand occurred from ~130 ka to ~115 ka, and studies from tectonically stable localities around the world indicate that sea level was substantially higher than present (by several meters) during this period (Muhs, 2002; Kopp et al., 2009; Murray-Wallace and Woodroffe, 2014; Dutton et al., 2015).

Despite general agreement that sea level was higher during the LIG, it has been known for more than 50 years that geologic records of this high-sea stand differ from coastline to coastline, even where tectonics have not played a role in bringing about measurable uplift or subsidence (Veeh, 1966). In some cases, these different records can be explained by the elevation uncertainties that are simply an inherent part of the geologic record. For example, the elevation of a shoreline angle (junction of a wave-cut platform with a sea cliff) of an erosional marine terrace may have uncertainties of only a meter or two. On the other hand, the height of an emergent reef, with fossil corals still in growth position, may provide a paleo-sea level indicator that is strictly a minimum estimate, as many species of corals can occupy water depths that range over tens of meters. Nevertheless, even where uncertainties in the nature of the geologic record can be ruled out, differences in paleo-sea level records are still substantial. On the tectonically stable coastlines of southern and western Australia, estimates of LIG paleo-sea level

range from ~2 m above present to ~4 m above present (O'Leary et al., 2013; Murray-Wallace et al., 2016). In contrast, estimates of LIG paleo-sea level from Brazil and the Seychelles Islands, also tectonically stable, range from ~8 to ~10 m above present (Veeh, 1966; Martin et al., 1988; Dutton et al., 2015).

It is now recognized that some of the differences between elevations of LIG marine deposits from coast to coast are likely due to glacial isostatic adjustment (GIA) effects (Hay et al., 2014). The deviation of an emergent shoreline's elevation from that expected from purely eustatic considerations will vary considerably, depending on the physical geography of the continent or island, the extent of continental or insular shelves, the distance from former continental ice sheets, and other variables (Dutton and Lambeck, 2012; Lambeck et al., 2012; Creveling et al., 2015; Dendy et al., 2017). Creveling et al. (2015) modeled the departure of LIG sea-level elevations from purely eustatic values for a large number of localities around the world, including the Bahamas and Bermuda. In conducting this modeling, Creveling et al. (2015) considered eustatic sea levels of both +6 m and +8 m, relative to present. These investigators modeled what LIG sea-level elevations could have been (including eustatic components) at both the start (set to ~127 ka) and the end (set to ~120 ka) of the LIG. Results of this study show that at the end of the LIG paleo-sea levels could have been as high as 11−13 m above present (at localities close to North American ice sheets) to as little as 5−8 m above present (at localities distant from North American ice sheets). Their results are similar in magnitude to those from modeling of LIG sea level presented by Dutton and Lambeck (2012) and Lambeck et al. (2012). Dendy et al. (2017) presented simulations of LIG sea level that considered how GIA modeling might be sensitive to different ice sheet volumes during the penultimate (MIS 6) glacial period, ~190-130 ka. Their results confirmed the hypothesis that different ice volumes during MIS 6 would have produced different sea-level responses during the LIG, but Dendy et al. (2017) also confirmed many of the earlier GIA modeling results reported by Dutton and Lambeck (2012), Lambeck et al. (2012) and Creveling et al. (2015). With regard to Northern Hemisphere regions close to the Laurentide Ice Sheet, such as the Bahamas and Bermuda, three findings are common to these modeling studies: (1) LIG sea level was likely higher than present, due to GIA processes as well as purely eustatic changes; (2) sea level was likely highest at the close of the LIG compared to the start of the LIG; and (3) LIG sea level would have been higher in Bermuda compared to the Bahamas.

These modeled findings provide a suite of hypotheses that can be tested using coastal geomorphology and U-series dating. Because the Bahamas and Bermuda are well north of the Caribbean-North American plate boundary (Fig. 1), it is reasonable to assume that coastlines on these islands have experienced little or no tectonic movement within the Quaternary. The purpose of the present study is to test the hypothesized, GIA-model-derived paleo-sea levels described above using the coastal geomorphic and stratigraphic record on the Bahamas and Bermuda. We use detailed elevation measurements combined with high-precision U-series dating to identify LIG sea-level markers and compare them to modeled values.

2. Methods

On New Providence Island in the Bahamas (Fig. 2), we examined exposures of emergent patch reefs and oolitic/peloidal beach ridge deposits mapped by Garrett and Gould (1984). All beach/sublittoral deposits examined were described for sedimentary structures and faunal compositions were determined for the patch reefs. Elevations of both beach ridges and patch reefs on New Providence Island were made using direct measurement by tape and hand level

(patch reefs) and/or by differential GPS measurements (beach ridges). GPS data were collected from at least four, and usually six to eight, satellites for at least 500 s to obtain consistent 3-D geometry. The data were postprocessed using corrections against the closest active base stations, utilizing the CARIB97 high-resolution geoid height model for the Caribbean Sea (Smith and Small, 1999). Differentially correcting the GPS elevations typically resulted in horizontal errors of 10 cm or less and vertical errors in the range of 20−80 cm. Comparison of GPS-derived elevation measurements with taped or hand-leveled elevation measurements and topographic map elevation measurements (contour interval 2 feet [0.61 m] for New Providence Island) shows good agreement, within the limits of instrumental and cartographic uncertainties. On Bermuda, most deposits are close enough to shore that simple tape and hand level measurements, with corrections for tidal variations, are sufficient for accurate elevation determinations.

On New Providence Island and Bermuda, only well-preserved corals were sampled in the field for U-series geochronology. Corals used were cleaned mechanically, washed in distilled water and X-rayed to estimate aragonite content. For X-ray diffraction (XRD) determination of the relative abundance of aragonite and calcite, we used heights of the prominent 26.2°, two-theta (aragonite) and 29.4°, two-theta (calcite) peaks; aragonite-to-calcite peak height ratios of samples were compared with a calibration curve of 18 artificial aragonite-calcite mixtures with aragonite contents ranging from ~2.5 to ~95% (Lowenstam, 1954). This simple calibration curve has been used to estimate aragonite and calcite contents by many carbonate petrologists over the years (Stanley, 1966; Veeh, 1966; Gupta, 1972; Magaritz et al., 1979; Somayajulu et al., 1985; Cohen and Branch, 1992; Dean et al., 2007; Dean, 2009), and was also utilized in all our previous studies of fossil corals (Ludwig et al., 1996; Muhs and Simmons, 2017; Muhs et al., 2002, 2011, Muhs et al., 2012b, Muhs et al., 2012c, 2014, 2017). Dean et al. (2007) more recently confirmed the validity of the Lowenstam (1954) curve in laboratories of the U.S. Geological Survey, using new artificial mixtures of aragonite and calcite and providing a mathematical expression of the calibration curve.

For beach ridge sediments, samples were taken for thin sections to determine relative abundances of ooids, peloids, and skeletal particles. Although most carbonate sediments in the Bahamas contain at least some particles from each of these three categories of carbonate grains, we report U-series data here for only those samples that are dominated by ooids and peloids. The reason for making this choice is that based on both early studies (Thurber, 1962) and more recent work (Chung and Swart, 1990; Muhs et al., 2011), ooids and peloids contain U derived from seawater when they precipitate as aragonite, in amounts ranging from about 2 to 4 ppm, similar to corals. Further, Muhs et al. (2011) reported that modern ooids from the Bahamas not only contain U, but the U in these particles has $^{234}U/^{238}U$ values of 1.1495−1.1496, identical to that of U in modern seawater (Chen et al., 1986; Delanghe et al., 2002). Thus, like corals, ooids and peloids are appropriate materials for U-series age determinations and reflect the time of ooid or peloid precipitation in the marine environment.

Chung and Swart (1990) found, consistent with earlier results presented by Kaufman et al. (1971), that mollusks and foraminifera, common as skeletal components in carbonate sediments, take up little or no U from seawater. Based on a thorough evaluation of the suitability of mollusks for U-series geochronology (Kaufman et al., 1971), it follows that molluscan-skeletal-dominated carbonate sediments will take up U secondarily, usually from terrestrial waters. Thus, at best, such materials provide only minimum ages, but they are also subject to later U loss or gain, making their apparent ages highly uncertain. Therefore, beach and sublittoral deposits on the Bahamas that are dominated by skeletal particles, which may

Fig. 1. Tectonic map of the Caribbean Basin and surrounding areas, showing faults (redrawn from Mann [2007] and Pindell and Kennan [2009]), lithospheric plates, directions of present plate movements (arrows), and localities referred to in text.

include mollusk and foraminifera fragments, were not utilized for U-series dating in the present study.

In studying oolitic sediments from the Florida Keys and the Miami area, Muhs et al. (2011) reported U-series data for untreated samples and splits from the same samples that had been treated with heavy liquid separations to remove calcite replacement products and calcite cement. In that study, calcite removal was undertaken with the assumption that secondary U loss (from calcite replacement of aragonite) or secondary U gain (from U coprecipitated with calcite cement) could have taken place. It was found that in untreated samples, U content was correlated in a positive linear fashion with aragonite content ($r^2 = 0.75$). Muhs et al. (2011) concluded from these data that calcite cement in these oolites may carry little or no U. These conclusions are consistent with fission track maps indicating an absence or low

concentrations of U in vadose calcite cement compared to adjacent ooids and peloids in sediments from the Bahamas (Chung and Swart, 1990; see their Fig. 3). Furthermore, although all samples studied by Muhs et al. (2011) showed some evidence of open-system behavior, based on back-calculated initial $^{234}U/^{238}U$ values, more-aragonite-rich splits obtained by heavy liquid separations actually showed more substantial open-system histories than bulk, untreated splits from the same samples. Hence, in the present study, we analyzed mostly untreated samples.

After cleaning of both corals and ooid/peloid sediments, sample preparation followed methods outlined by Ludwig et al. (1992), summarized briefly here. Cleaned corals and ooid/peloid samples were dissolved in HNO_3, spiked with ^{229}Th, ^{233}U, and ^{236}U and purified with ion exchange methods. Purified U and Th were loaded with colloidal graphite on separate Re filaments and isotopic
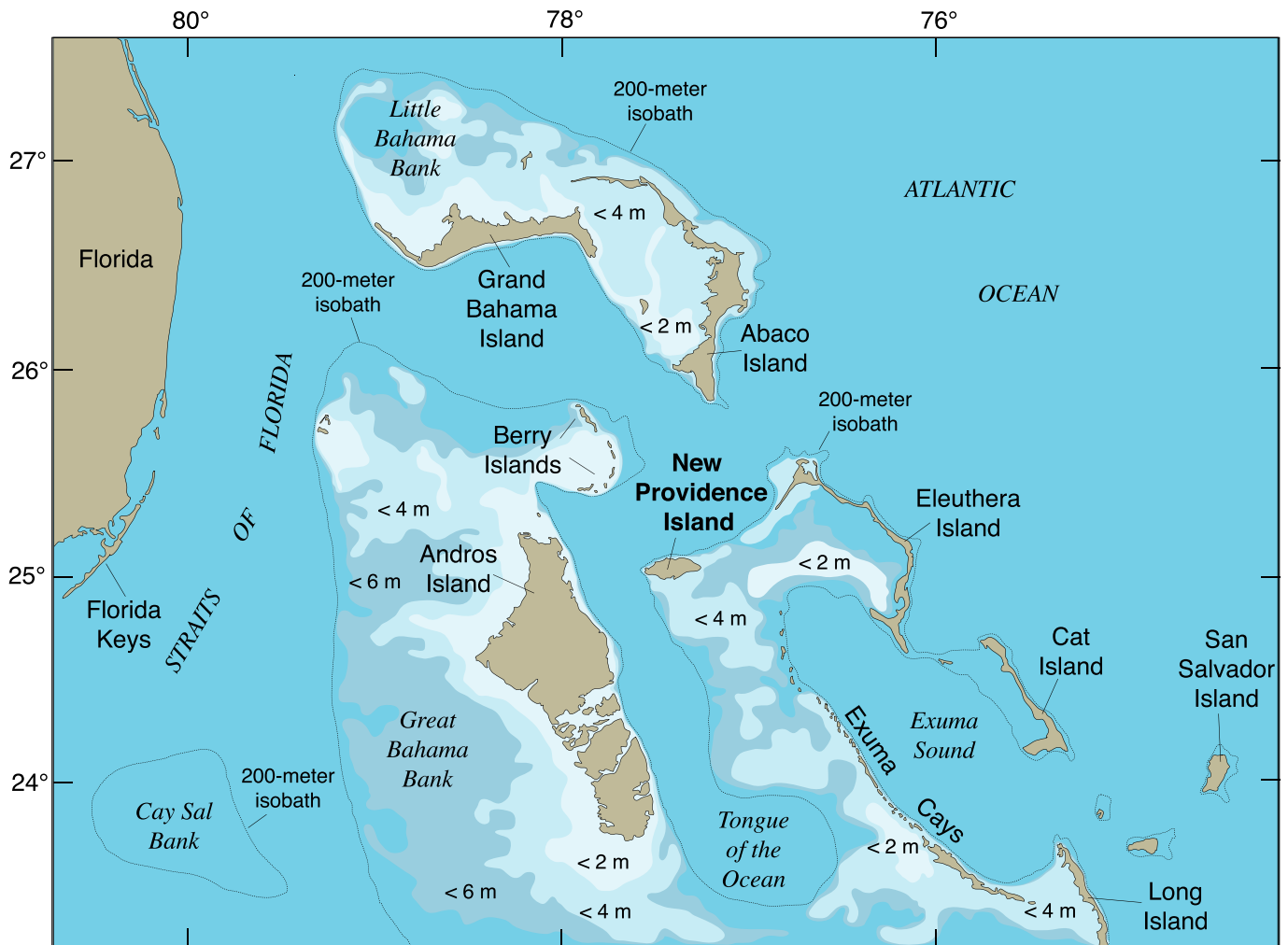
Fig. 2. Map showing the islands of the Bahamas, the location of New Providence Island, and the approximate depths of the banks on which the islands are situated. Depth data simplified from hydrographic chart published by the Government of the Commonwealth of the Bahamas, 1988.

abundances were determined by thermal ionization mass spectrometry (TIMS). The U—Th spike is calibrated against a solution of uranium ore from the Schwartzwalder Mine that has yielded concordant U/Pb ages (Ludwig et al., 1985) and sample-to-sample agreement of $^{234}U/^{238}U$ and $^{230}Th/^{238}U$ (Ludwig and Paces, 2002). In addition, an in-house, carefully homogenized, aragonitic fossil coral of last interglacial age (~120 ka) was used for run-to-run checks. Ages were calculated using a half-life of 75,584 yr for ^{230}Th and a half-life of 245,620 yr for ^{234}U (Cheng et al., 2013).

Alternative age calculations were also performed using the open-system "correction" scheme of Thompson et al. (2003). This method of age calculation is based on the observation by Gallup et al. (1994) that corals yielding back-calculated $^{234}U/^{238}U$ values (based on their ages and measured $^{234}U/^{238}U$ values) higher than modern seawater tend to be biased to older apparent ages. Although there is uncertainty as to how universally applicable this method is for calculations of "open-system" ages (see review in Stirling and Andersen, 2009), the approach certainly provides an empirically based, quantitative protocol for considering alternative age estimates. Thompson et al. (2003) note that the open-system correction method should not be applied to coral samples with excessively high apparent initial $^{234}U/^{238}U$ values and/or excessively high amounts of ^{232}Th.

3. Geology of New Providence Island

The islands of the Bahamas are situated on broad, shallow carbonate platforms. These carbonate banks are less than 6 m deep and in many places are less than 4 m deep (Fig. 2). Basins between the shallow carbonate shelves on which the islands are located are hundreds to thousands of meters deep. Based on cores taken west of Andros Island (Fig. 2), Great Bahama Bank is underlain by carbonate sediments that are at least 600 m thick and are likely of Miocene age at this depth (Melim and Masaferro, 1997). Miocene sediments are in turn overlain by Pliocene and Quaternary sediments. The subaerial parts of the islands are composed dominantly of Pleistocene and Holocene carbonate sediments. The topographically highest parts of the islands (~7 m high or higher) are eolianites. Topographically lower parts of the Bahamas (less than ~7 m above sea level) host beach, reef, intertidal, and subtidal sediments (Carew and Mylroie, 1997). Interdune lowlands contain lakes in places. Virtually all of the subaerially exposed sediments are carbonates. The only notable exceptions to this generalization are the modern soils and paleosols, which have received substantial contributions of fine-grained silicate minerals from long-range-transported African dust (Muhs et al., 1990, 2007).

The geology of New Providence Island is similar to that of most islands in the Bahamas. This island is composed largely of
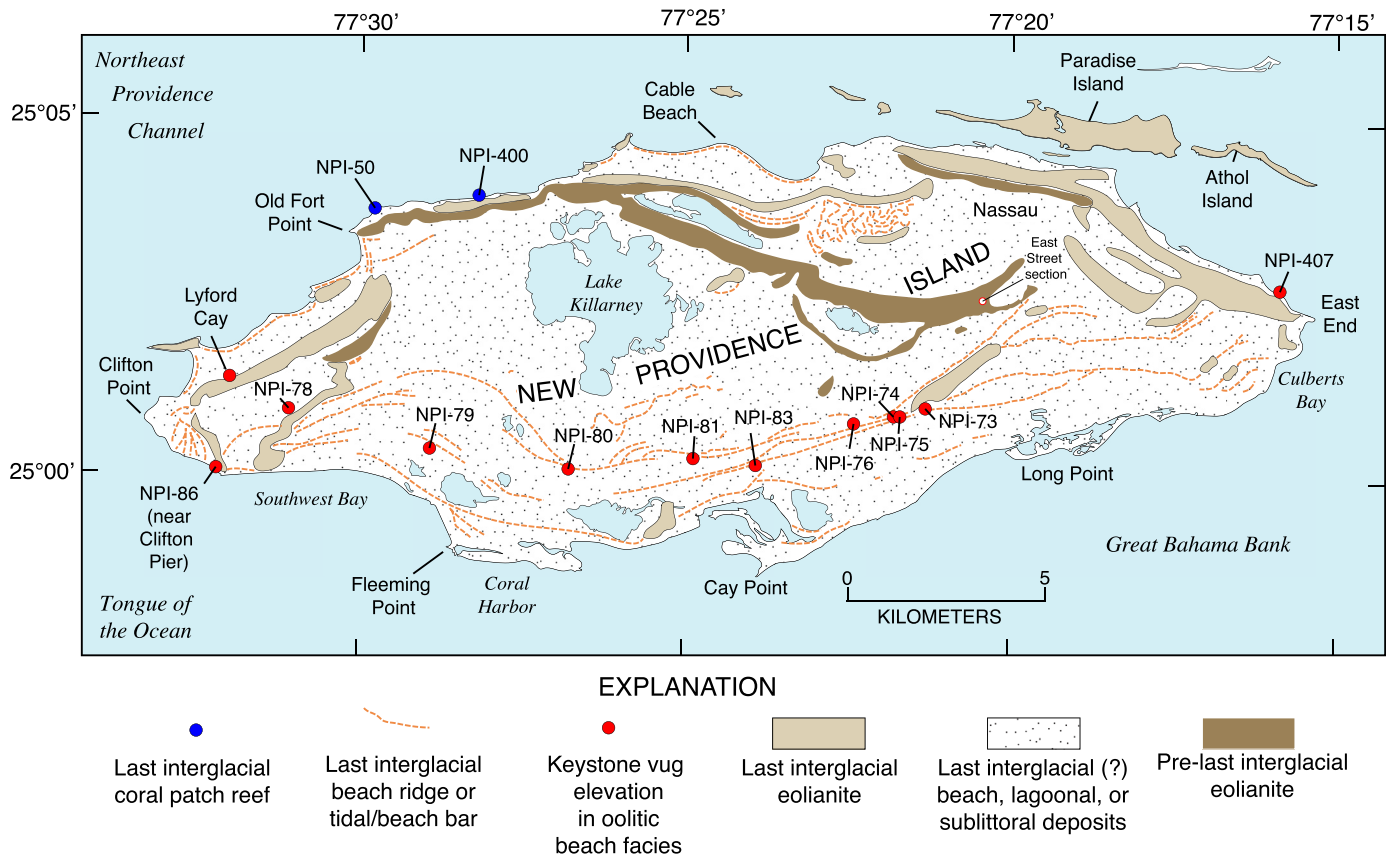
Fig. 3. Map of New Providence Island, Bahamas, showing surficial geology and the locations of study sites. Redrawn in modified form from Garrett and Gould (1984).

carbonate eolianite, marine sands, beach sands, coral-dominated patch reefs, and tidal flat sediments, all of Quaternary age. Garrett and Gould (1984) provided the first geologic map of New Providence Island and our own field work, conducted on five trips to the island, confirms the mapping that these investigators presented (Fig. 3). Hearty and Kindler (1997) studied the geology of the island later and their work also confirms the original mapping of Garrett and Gould (1984).

On New Providence Island, the majority of sediments we examined consist of peloids and ooids, and ooids often have a peloid nucleus (Fig. 4). Less commonly, skeletal fragments from corals, mollusks, foraminifera, and echinoderms form the majority of carbonate particles. Many ooids show a single suite of parallel, concentric aragonite coatings around a peloid nucleus. Another variation, however, is formation of an ooid with a peloid nucleus, followed by coalescence of two or more ooids with peloid nuclei into a compound grain with new aragonite coatings around two or more grains (Fig. 4). Calcite cement binds these particles into a calcarenite.

There is a distinctive change in facies of modern carbonate sediments on the Bahamas in a seaward-to-landward direction (see reviews in Halley et al., 1983 and Strasser and Davaud, 1986). Patch reefs are found offshore, typically in waters a few meters deep. Sublittoral sands are also found in shallow water. Moving shoreward, beach sands are found in the intertidal swash zone and landward of beaches, eolian sands are the dominant deposits.

Emergent, fossil patch reefs were reported by Garrett and Gould (1984) on New Providence Island at a number of localities. In the course of our field work, we found only two such features, both on the north side of the island (Fig. 3). At both localities (NPI-50 and NPI-400), patch reefs consist of coastal outcrops with a shore-

normal extent of ~10 m (Fig. 5a). Within these reefs, we found colonies of *Acropora cervicornis*, *Orbicella* sp. (cf. *O. annularis*), and *Diploria* sp., many of which are in growth position (Fig. 5b, c, d). Mollusks are present in these deposits as well.

Landward of fossil patch reefs, cemented carbonate sands from the sublittoral zone, characterized by wave ripples, often oblique to one another, can be found. In cross section, these sands show small-scale, trough cross-bed sets (Fig. 6a and b). Beach face deposits, also usually cemented, but initially formed within the intertidal zone or swash zone, are found landward or above sublittoral sands. Beach sediments typically show low-angle (5–15°) dips in a seaward direction. One distinctive aspect of emergent, fossil beach-face deposits in the Bahamas is the presence of what are called "keystone vugs" or "beach fenestrae" (Inden and Moore, 1983), voids with diameters of a few millimeters, that often have a circular to keystone shape (Fig. 6c). These vugs form from trapped air bubbles in the active swash zone. Because of the rapid rate (1000 yr or less) with which carbonate sediments on the Bahamas can be cemented (Halley and Harris, 1979), keystone vugs can be preserved in emergent, cemented beach sediments. Formation of vugs in the swash zone makes these features particularly valuable as paleo-sea-level indicators. Landward of the beach face deposits are back-beach or supratidal sediments, composed of beds that are horizontal or have very low-angle, seaward dips.

The most-landward carbonate facies in the Bahamas are typically eolian sands. Eolian sands are mostly of Pleistocene age, although Holocene eolian sands have been reported as well. Both ages of sediments have been cemented, to a greater or lesser degree, into eolianite. On New Providence Island, Garrett and Gould (1984) showed that eolianites are situated landward of supratidal (back beach) or beach face deposits. Eolianites on this island form
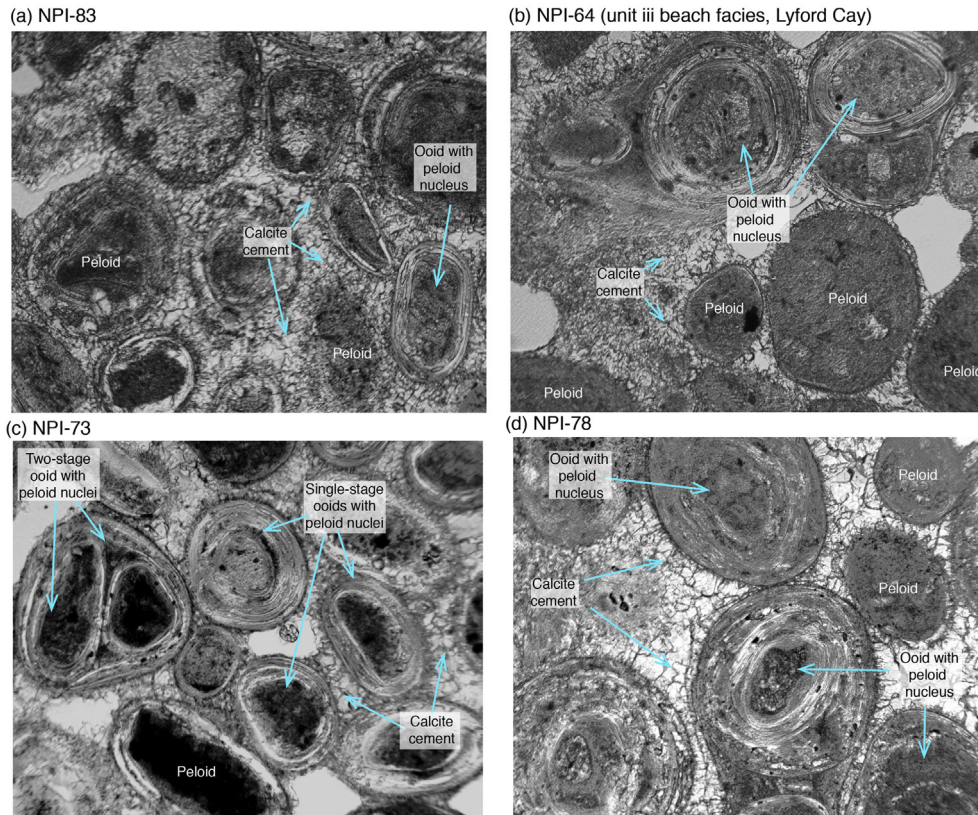
Fig. 4. Thin section photomicrographs of samples NPI-83 (Fig. 3), NPI-64 (=unit "iii", beach facies at Lyford Cay, Fig. 7), NPI-73 (Fig. 3), and NPI-78 (Fig. 3) showing sand-sized ooids, peloids, and compound (two-stage) ooids with peloid nuclei, and calcite cement. Scale: ooids and peloids on NPI have diameters of ~0.5 to~1.5 mm. All photographs by D.R. Muhs.

prominent ridges that are, topographically, the highest parts of the landscape (Fig. 3). The oldest, inland eolianite ridges have elevations as high as ~33 m above sea level. Muhs et al. (1990, 2007) reported alpha-spectrometric U-series ages of ~352 to ~310 ka for ooids in one of these older ridges, on East Street, south of Nassau (Fig. 3). Eolianite ridges thought to date to the last interglacial period (Garrett and Gould, 1984) are found seaward of these older, higher ridges and have maximum elevations of ~25 m. Eolianites have low-angle (~10°−15°) topset beds that dip upwind and high-angle (~25°−35°) foreset beds that dip downwind (Fig. 7).

An important aspect of eolianite stratigraphy on New Providence Island is the presence of paleosols between sedimentary units (Fig. 7). Paleosols developed within eolianites have the following characteristics: (1) obliterated primary structures; (2) light grey, pink, or very light reddish-brown colors; (3) substantial amounts of non-carbonate clay particles; (4) platy calcretes (K horizons), often fragmented; (5) rhizoliths; and (6) land snails, species of the genus *Cerion*. The pink or reddish colors and accumulated clay are due to inputs of long-range-transported dust from Africa (Muhs et al., 2007).

One of the best-studied exposures of the beach-to-eolianite facies transition is an extraordinary roadcut at Lyford Cay (Fig. 3), in western New Providence Island (Garrett and Gould, 1984; Muhs et al., 1990, 2007; Hearty and Kindler, 1997). Here, six eolianite/beach units are exposed in a roadcut more than 180 m long that displays more than 10 m of section (Fig. 7). Garrett and Gould (1984) numbered these units "i" to "vi," from oldest to youngest, a nomenclature retained by Muhs et al. (1990, 2007) and Hearty and Kindler (1997), and used here as well.

The oldest unit ("i") is an eolianite dominated by skeletal particles based on thin section examination. In this unit, topsets dip

15°−20° to the north and foresets dip 22°−32° to the south. Muhs et al. (1990, 2007) reported U-series ages of ~200 ka for aragonite separates of unit "i", but the dominance of skeletal particles in this bed makes these age estimates highly tentative. A reddish-brown paleosol, ~40 cm thick, with *Cerion* land snails, has developed in the upper part of unit "i" and separates this unit from the overlying unit "ii".

Unit "ii", where it is exposed in the northern part of its extent, has both beach and eolian facies. The beach beds dip ~3° to the north and have a maximum thickness of ~50 cm, grading to zero to the north, where they disappear under the road. Vugs are present in the upper part of these beds, at an elevation of 10.7 m above sea level. The beach sediments of unit "ii" appear to lap onto a thick eolianite (Fig. 7). The eolianite has topset beds that in turn grade, farther south, into foreset beds with high-angle (25°−31°) southward dips and an overall thickness of ~9−10 m. If our interpretation is correct, the thick eolianite of unit "ii" predates the beach facies of unit "ii", which laps onto it from the north.

Still farther north, Garrett and Gould (1984) reported a younger sediment body, their unit "iii," onlapping unit "ii", also with both a beach and eolianite facies (Fig. 7). We also recognize this unit, although there is no paleosol between units "ii" and "iii," indicating either erosion of any preexisting soil on unit "ii" or very little time between the deposition of the two units. The beach facies of unit "iii" is ~1.8 m thick, has beds that dip 2°−5° to the north, and contains vugs at an elevation of 11.8 m. The eolianite facies ranges in thickness between 2.3 and 2.6 m, has northward-dipping topset beds at its northward side and high-angle (24°−34°) foreset beds, dipping south. As is the case with unit "ii," we hypothesize that the beach facies of unit "iii" onlaps the eolianite facies of unit "iii," postdating it slightly. Both beach and eolianite facies of units "ii"
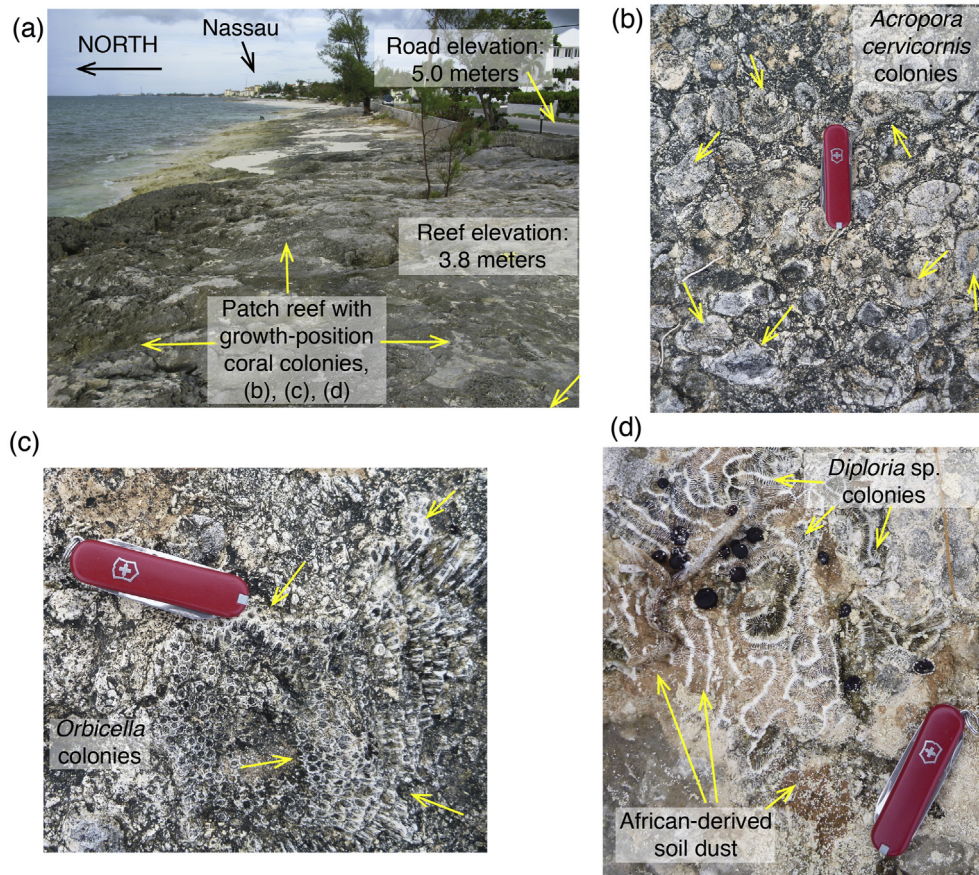
Fig. 5. Patch reef at locality NPI-400 (see Fig. 3): (a) reef extent and elevations; (b) *Acropora cervicornis* corals in growth position; (c) *Orbicella* sp. corals in growth position; (d) *Diploria* sp. colony, probably in growth position, along with infiltrated African soil dust (red colors). Knife for scale in (b), (c), and (d) is 5.5 cm long; all photographs by D.R. Muhs. (For interpretation of the references to color in this figure legend, the reader is referred to the Web version of this article.)

and "iii" are dominated by ooids and peloids with only rare skeletal particles. Muhs et al. (1990, 2007) reported alpha-spectrometric U-series ages of ~129 to ~114 ka for ooids and peloids of unit "ii" and ~131 to ~118 ka for ooids and peloids of unit "iii."

In the upper part of the Lyford Cay section, units "iv," "v," and "vi" are all eolianites with high-angle foreset beds dipping to the south. They are separated from one another and from the underlying units "ii" and "iii" by minimally developed paleosols that all contain *Cerion* land snails. Whereas units "iv" and "v" are dominated by ooids and peloids (about equal numbers of both) and only rare skeletal fragments, unit "vi" is dominated by peloids and skeletal fragments, with only rare ooids. All ooid-peloid-dominated units (units "ii,", "iii," "iv," and "v"), both marine and eolian facies, were sampled for U-series geochronology.

4. Geology of Bermuda

The geology of Bermuda was first studied in detail by Sayles (1931), who identified many of the salient features of the island's Quaternary geology. It was Sayles (1931), in fact, who coined the term "eolianite" to describe the cemented carbonate dune ridges that, like the Bahamas, dominate the surficial geology of this island. Eolianite ridges of Bermuda are situated atop a volcanic pedestal. Depths to volcanic rocks average ~45 m below sea level in western and central Bermuda and ~30 m below sea level in eastern Bermuda. Modern geologic maps of Bermuda, as well as detailed descriptions of the island's sediments and their origins are found in Vacher et al. (1989, 1995), Rowe (1990), and Vacher and Rowe

(1997). These studies have shown that there are six major carbonate eolianite units, separated by paleosols, that compose the island's Pleistocene deposits. These are, from oldest to youngest, the Walsingham Formation, Town Hill Formation (with lower and upper members), Belmont Formation, Rocky Bay Formation (which includes the Devonshire marine member), and the Southampton Formation (Fig. 8). There are only rare occurrences of marine deposits associated with the Walsingham Formation and both members of the Town Hill Formation, as these units are dominated by eolianite. These older units host well developed, clay-rich, red soils in their upper parts (see examples in Muhs et al., 2012a). The younger Belmont, Rocky Bay, and Southampton Formations are also dominantly eolianite, but all three have numerous localities with sediments of a marine facies. Corals from the marine facies have been crucial in developing a chronology for the Pleistocene of Bermuda, as discussed below.

Rowe (1990), Vacher et al. (1995), Vacher and Rowe (1997), Rowe et al. (2014), and Rowe and Bristow (2015) have provided detailed interpretations of the shallow marine and eolian facies on Bermuda. Bermudan carbonate facies are similar in some respects to those on the Bahamas, at least for some ages of deposits, such as the ~200 ka Belmont Formation (Rowe et al., 2014). A notable difference between carbonate sediments on the Bahamas and Bermuda, however, is that whereas Bahaman sands are composed dominantly of ooids and peloids, with minor skeletal components, Bermudan sands are composed almost entirely of sandy skeletal particles. In the Belmont Formation, upper shoreface oscillation ripples, upper shoreface beach step, and foreshore beach face
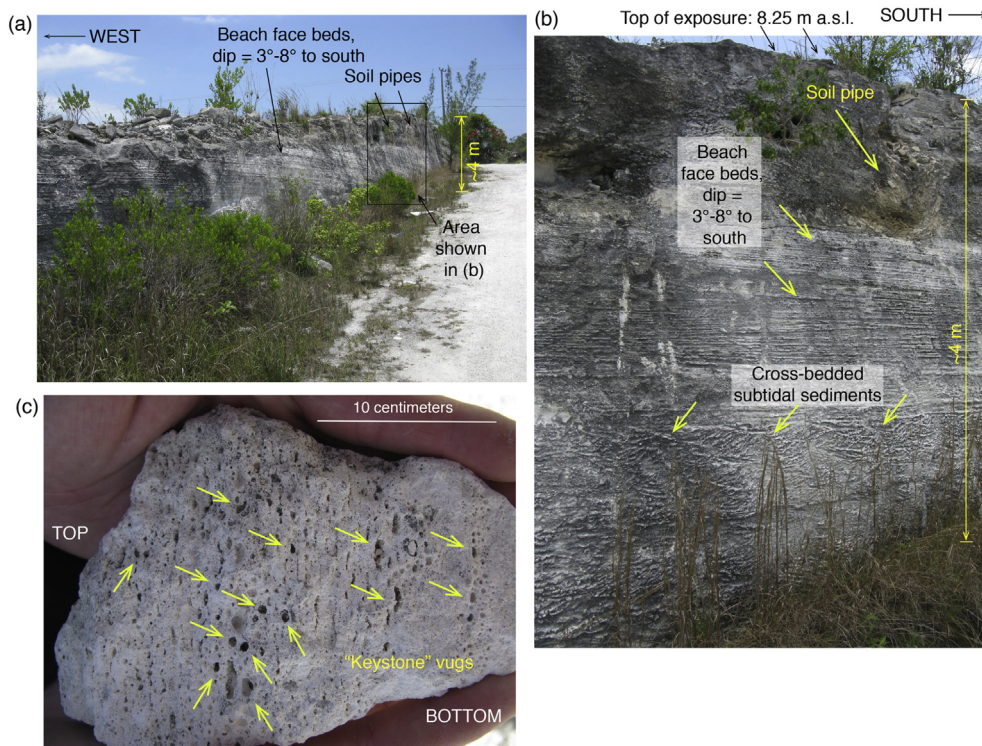
Fig. 6. Photographs of beach ridge and structures at localities NPI-83 and NPI-78 (see Fig. 3): (a) NPI-83 roadcut exposure; (b) NPI-83 beach ridge structures: cross-bedded subtidal sands, beach face beds, soil pipe. (c) NPI-78: closeup photograph of subhorizontal beach face beds with keystone vugs or beach fenestrae. All photographs by D.R. Muhs.

deposits are all well displayed in coastal outcrops (see Rowe et al., 2014, their Fig. 5). A well-developed, reddish-brown, clay-rich paleosol, called the Shore Hills "Geosol" (Vacher and Rowe, 1997) developed on the Belmont Formation (both marine and eolian facies) and separates the Belmont from the overlying Devonshire marine member or the Rocky Bay Formation (eolianite), of LIG age (Harmon et al., 1983). Where the Belmont Formation is exposed on the southern coast of Bermuda, the Shore Hills paleosol that separates it from the younger, overlying Devonshire marine member is mostly eroded, but reddish-brown, clay-rich soil pipes are found in solution hollows of the Belmont (see Fig. 7 of Muhs et al., 2012a, for examples of soil pipes in an older unit on Bermuda). These Shore Hills paleosol pipes are important for reconstructing sea level history, because their presence implies a period of sea-level lowering and subaerial exposure between the time of Belmont Formation deposition and sedimentation of the overlying Devonshire marine member of the Rocky Bay Formation.

The Devonshire marine member of the Rocky Bay Formation exhibits discernible but cruder bedding than the Belmont Formation. Where we have observed it, the Devonshire marine member consists largely of poorly sorted, mollusk- and coral-bearing carbonate sand and gravel resting on wave-cut benches or deposited in notches, where they unconformably overlie better cemented and stratified deposits of the Belmont Formation (Fig. 9). At Grape Bay, skeletal sands in the Devonshire marine member of the Rocky Bay Formation consist of seaward-dipping (5°–17° to the south) beds alternating with landward-dipping beds at somewhat higher (10°–18°) angles. Meischner et al. (1995) interpret the relatively high-angle landward dips at Grape Bay to be the result of slumping. Devonshire marine beds in the Grape Bay area, where they are well exposed, vary in thickness from ~0.45 m to as much as ~3.4 m. All the beds in this area exposed near the coast were interpreted to be sublittoral or beach sands by Meischner et al. (1995), and we agree with that interpretation.

Bivalves, gastropods, and corals are found within all beds, but mollusks and corals are particularly abundant at the base of the Devonshire, just above the bench cut on the underlying Belmont Formation. Notable among the molluscan assemblage is the large gastropod *Cittarium pica*, which is abundant in all exposures we found at Grape Bay. Bivalves observed include *Lucina*, *Glycymeris*, and *Arca*. In places (e.g., Coco Reef, Rocky Bay, and occasionally at Grape Bay; see below), corals appear to be in growth position within Devonshire deposits, but at most localities, corals are wave-worn gravel clasts within a poorly sorted sandy matrix (Fig. 10). Coral taxa observed include *Orbicella* sp. or spp., *Diploria strigosa*, *Montastraea cavernosa*, *Siderastrea* sp. or spp., and *Oculina* sp. or spp.

Eolianites on Bermuda have been studied extensively (Sayles, 1931; Mackenzie, 1964a, Mackenzie, 1964b; Land et al., 1967; Vacher et al., 1989; Rowe and Bristow, 2015). These deposits exhibit landward-dipping foreset beds at high (25–35°) angles (Fig. 9a) and seaward-dipping topset beds at low (5–10°) angles. As is the case on the Bahamas, eolian deposition on Bermuda was episodic, separated by periods of landscape stability, indicated by the presence of paleosols. On Bermuda, paleosols developed on eolianite are better developed than those on the Bahamas, with thick, red or reddish-brown colors, and considerable clay accumulation. Similar to paleosols on the Bahamas, paleosols on Bermuda developed primarily from inputs of long-range-transported dust from Africa, but weathering of small amounts of volcanic particles from the island's subsurface has also contributed to soil genesis (Muhs et al., 2012a).

Corals in the marine facies of the younger formations of Bermuda have been essential to establishing a chronology for the island. Whereas Hearty (2002) estimated the Belmont Formation to be of LIG age (MIS 5.5), based on amino acid ratios in fossil mollusks, three different studies have shown that corals from the marine facies of the Belmont Formation date to the penultimate
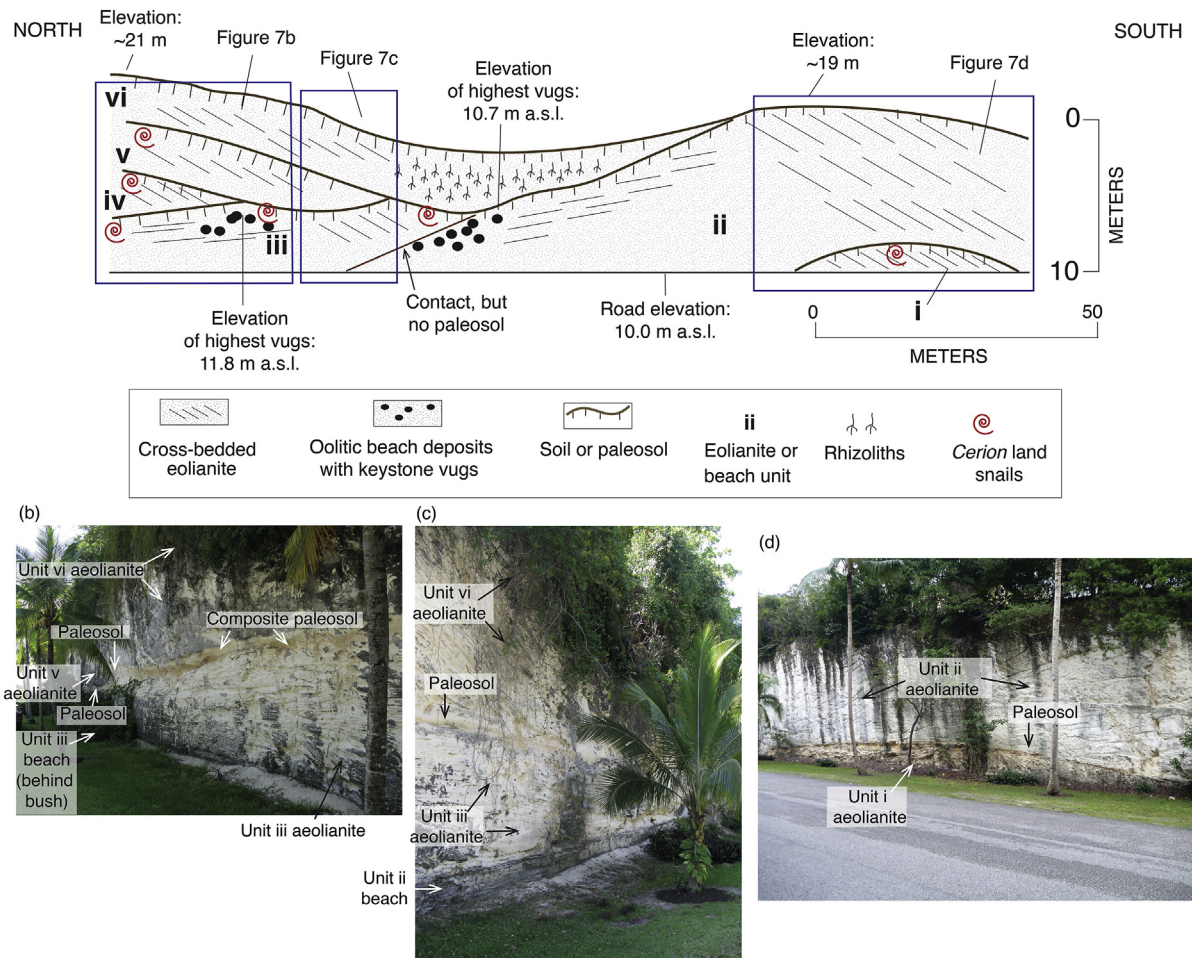
Fig. 7. (a) Stratigraphy of beach and eolianite deposits and GPS-derived beach elevations at Lyford Cay, New Providence Island (Fig. 3), redrawn in slightly modified form from Garrett and Gould (1984). Note that thicknesses of some units are slightly enlarged for clarity; (b), (c) Photographs of units exposed on the northern side of the roadcut (see (a) for location). (d) Photograph of the oldest eolianite unit, on the southern side of the roadcut (see (a) for location). All photographs by D.R. Muhs.

interglacial period (MIS 7), at ~200 ka (Harmon et al., 1983; Muhs et al., 2002; Rowe et al., 2014). The younger Devonshire marine member of the Rocky Bay Formation hosts a number of species of corals (Fig. 10) and ages of these specimens range from ~126 to ~114 ka, correlating this unit with MIS 5.5 (Harmon et al., 1983; Muhs et al., 2002). Marine deposits of the Southampton Formation, exposed at Fort St. Catherine (Fig. 8), contain abundant fragments of the coral *Oculina* (Fig. 10a). Ages of *Oculina* fragments at Fort St. Catherine range from ~84 to ~78 ka, correlating this unit with MIS 5.1 (Harmon et al., 1983; Ludwig et al., 1996; Muhs et al., 2002).

5. Uranium-series dating of corals and oolites

5.1. U-series ages of fossil corals

In assessing the integrity of U-series coral ages reported here, we consider several criteria, established during the early years of U-series geochronology by Broecker and Thurber (1965) and still valid today. These include: (1) absence of recrystallization of primary aragonite to calcite, based on both examination of samples under magnification and XRD analyses; (2) verification that ^{230}Th measured is due to in situ radioactive decay of parent ^{234}U and not from detrital silicate contaminants, confirmed by low concentrations of ^{232}Th and high values of ^{230}Th/^{232}Th; (3) verification that bulk U concentrations are within the range of modern samples of

the same species, indicating that there has been no gain or loss of U since deposition; and (4) measured ^{234}U/^{238}U values that, when combined with apparent ^{230}Th/^{234}U ages, yield back-calculated initial ^{234}U/^{238}U values that fall within the range of modern seawater.

Here we assess the integrity of our coral analyses with the criteria outlined above in mind. Based on XRD, all corals we analyzed from both New Providence Island and Bermuda are 95−100% aragonite (Table 1), indicating no substantial recrystallization. High ^{232}Th concentrations (and therefore low ^{230}Th/^{232}Th values) are measures used to indicate significant inherited ^{230}Th from detrital silicate minerals. High values for these two measures will indicate probable bias to older apparent ages. The choice of what ^{232}Th concentration or which ^{230}Th/^{232}Th value to use as a threshold for determining whether or not there is significant detrital mineral contamination is typically chosen by individual laboratories. Among the samples considered here, only two (NPI-50-G-1 and NPI-50-H-1, both specimens of *Acropora cervicornis*) have any substantial amount of ^{232}Th, both ~0.03 ppm, with ^{230}Th/^{232}Th values < 300. All other samples have very low concentrations of ^{232}Th (0.02 ppm or less, with all but one 0.005 ppm or less), and ^{230}Th/^{232}Th values that range from ~2700 to ~12,000.

U-series geochronologists sometimes overlook criterion (3), bulk U content of fossil corals, in their interpretations. However, secondary additions of bulk U will bias samples to younger
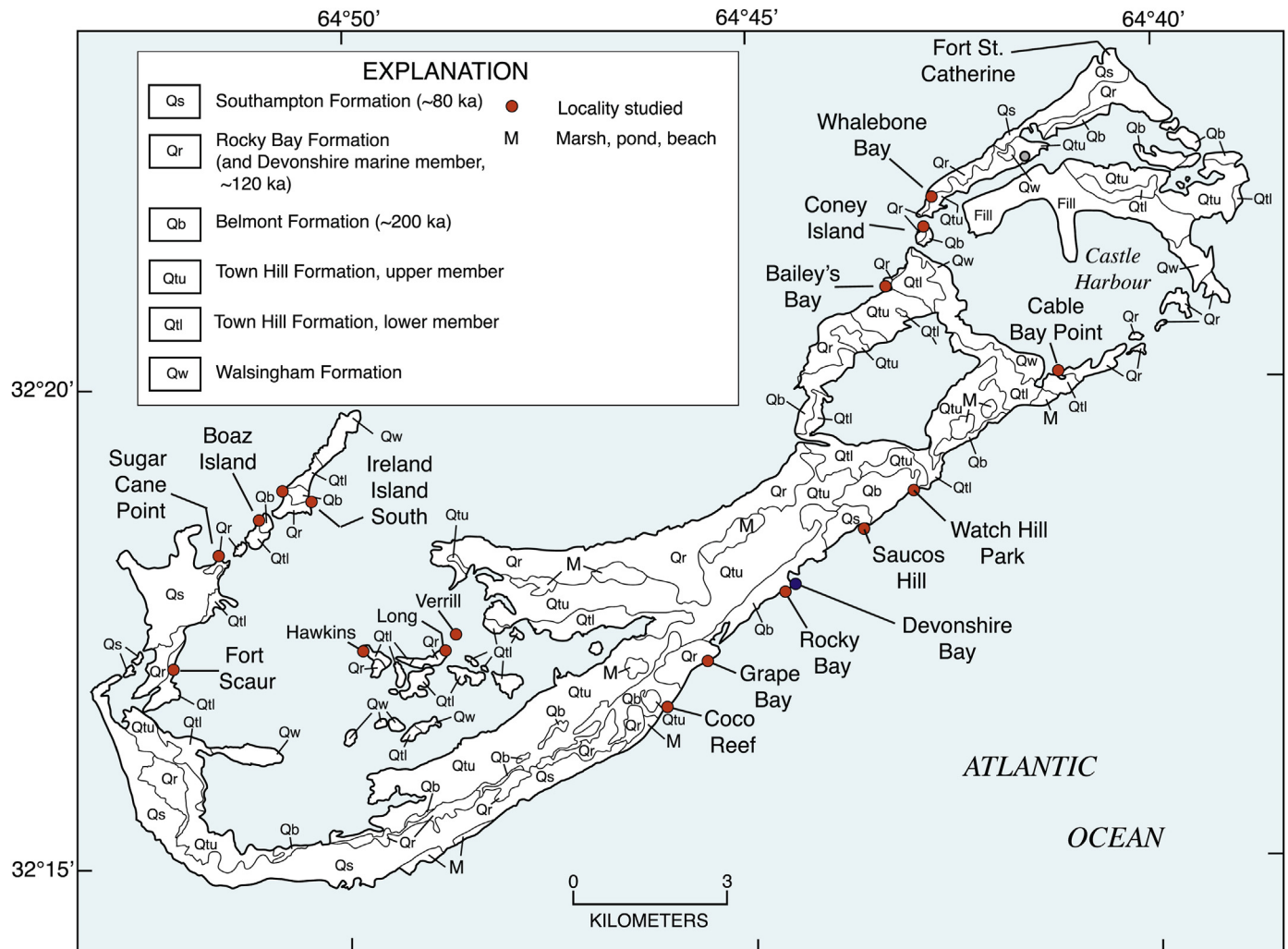
Fig. 8. Geologic map of Bermuda (redrawn in simplified form from Vacher et al., 1989). Filled red circles show marine deposit localities of the Devonshire marine member of the Rocky Bay Formation, dated or correlated to the last interglacial period (~120 ka), where elevations were measured. (For interpretation of the references to color in this figure legend, the reader is referred to the Web version of this article.)

apparent ages and U loss will bias samples to older apparent ages. Modern and Holocene specimens of *Orbicella*, *Siderastrea*, *Diploria*, and *Porites* have U concentrations of 2–3 ppm (Cross and Cross, 1983; Chen et al., 1991; Ludwig et al., 1996; Muhs et al., 2011, 2017). Fossil specimens of *Siderastrea* with apparent closed-system histories sometimes have U contents slightly higher than 3 ppm (Martin et al., 1988; Gallup et al., 2002; Speed and Cheng, 2004; Muhs et al., 2014, 2017). In contrast, modern and Holocene species of *Acropora* (*A. palmata* and *A. cervicornis*) consistently have U concentrations of 3.0–3.8 ppm (Cross and Cross, 1983; Chen et al., 1991; Gallup et al., 1994; Thompson et al., 2011). In the suite of samples presented here, the same two problematic specimens described above, NPI-50-G-1 and NPI-50-H-1 (*Acropora cervicornis*), have U concentrations of 2.6 and 2.89 ppm, respectively, indicating bulk U loss (despite no recrystallization of NPI-50-H-1). Because of the evidence for both U loss and detrital Th in these two samples, we do not use the apparent ages of these specimens in our interpretations. The remaining samples have U concentrations of 2.54–2.75 ppm, which are within the range of U found in modern specimens of *Orbicella*, *Diploria*, and *Siderastrea* (Table 1).

The best criterion for determining closed-system conditions during the post-emergence history of a fossil coral is concordance between $^{230}Th/^{234}U$ and $^{231}Pa/^{235}U$ ages (Edwards et al., 1997;

Gallup et al., 2002; Cutler et al., 2003). We did not determine $^{231}Pa/^{235}U$ ages for our samples, nor do most U-series laboratories because of the difficulties in using the ^{233}Pa spike that is required (see discussion in Hibbert et al., 2016). However, another measure for closed-system history, criterion (4) given above, is a determination of whether the back-calculated initial $^{234}U/^{238}U$ value of a sample, based on its present measured $^{234}U/^{238}U$ value and the $^{230}Th/^{234}U$ age, is within the range of modern seawater. Modern seawater, commonly cited as having an "average" $^{234}U/^{238}U$ value of 1.149, actually has a significant range of values, from 1.140 to 1.155 (Chen et al., 1986; Delanghe et al., 2002). Modern corals from Caribbean beaches reflect this range of values. In southern Cuba, for example, modern corals have $^{234}U/^{238}U$ values ranging from 1.143 to 1.152 (Muhs et al., 2017).

Evaluation of back-calculated initial $^{234}U/^{238}U$ values has become, within the U-series geochronology community, the de facto measure for assessing closed-system history of fossil corals. Gallup et al. (1994) pointed out that corals with elevated initial $^{234}U/^{238}U$ values from within the same reef terrace tend to yield older apparent ages. On a $^{230}Th/^{238}U$ vs. $^{234}U/^{238}U$ evolution diagram, such samples will plot above a theoretical isotope evolution pathway. A number of corals from New Providence Island and Bermuda show only minimal evidence of open-system histories by
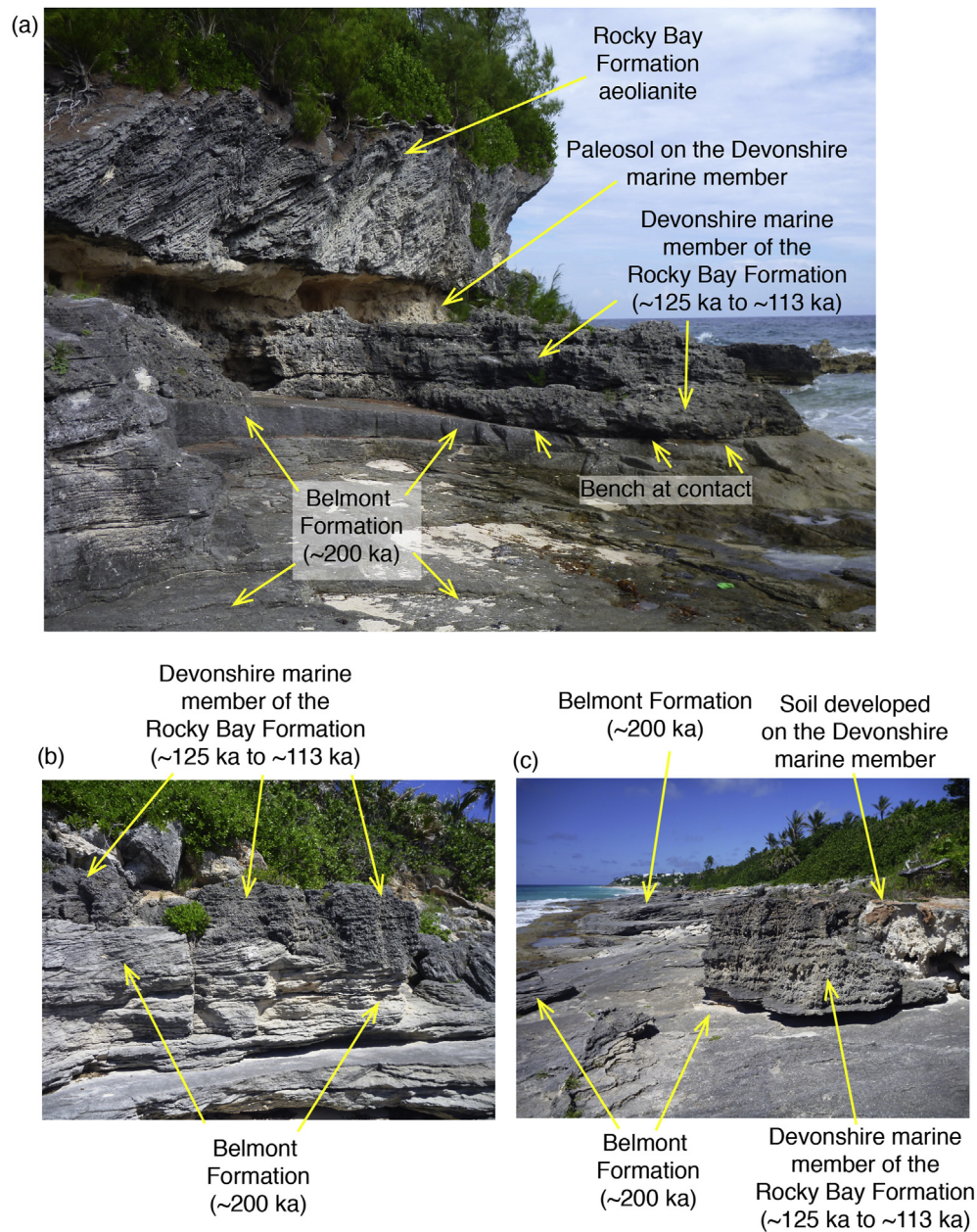
Fig. 9. Stratigraphy of marine and eolian deposits on Bermuda. (a) Rocky Bay, Bermuda (see Fig. 8 for location), showing Belmont Formation marine facies, dated to ~200 ka (Harmon et al., 1983; Muhs et al., 2002; Rowe et al., 2014); Devonshire marine member of the Rocky Bay Formation, dated to ~120 ka (Harmon et al., 1983; Muhs et al., 2002); weakly developed paleosol on the Devonshire marine member; and eolianite facies of the Rocky Bay Formation. (b) View of the Belmont Formation and Devonshire marine member of the Rocky Bay Formation, a short distance southwest of Grape Bay (see Fig. 8 for location). (c) View to the southwest from Grape Bay, showing Belmont Formation, Devonshire marine member of the Rocky Bay Formation, and remnant of surface soil developed on the Devonshire, exposed at Grape Bay. All photographs by D.R. Muhs.

this criterion (Fig. 11a), with back-calculated initial $^{234}U/^{238}U$ values ranging from ~1.141 to ~1.158 (Table 1). We consider these corals to have only minor possible age bias. In contrast, many corals from the nearby Florida Keys, reported by Muhs et al. (2011), display the tendency described by Gallup et al. (1994), with numerous open-system histories, but with a roughly linear trend towards a closed-system age of ~120 ka (Fig. 11b).

For the New Providence Island corals from patch reefs or coral-bearing marine sediments, those with back-calculated initial $^{234}U/^{238}U$ values ranging from ~1.145 to ~1.158 have an age range of ~128 to ~118 ka, corresponding to the LIG, or MIS 5.5 (Table 1). Four newly collected corals from the Devonshire marine member on Bermuda have initial $^{234}U/^{238}U$ values ranging from ~1.141 to ~1.154

and an age range from ~118 to ~114 ka. We also recalculated ages of corals from this same marine unit (all collected at Grape Bay) reported by Muhs et al. (2002), using the newer estimates of half-lives of ^{230}Th and ^{234}U reported by Cheng et al. (2013). We omitted two samples reported in that study, both specimens of *Oculina*, that showed clear evidence of U loss. The remaining samples have initial $^{234}U/^{238}U$ values ranging from ~1.148 to ~1.156 and newly calculated ages ranging from ~126 to ~114 ka, in broad agreement with the corals from New Providence Island.

Despite the evidence for mostly closed-system histories of several corals from New Providence Island and Bermuda (Fig. 11a), there is potentially still some bias to slightly older ages based on somewhat higher-than-ideal, back-calculated initial $^{234}U/^{238}U$

Fig. 10. Examples of corals in marine deposits of Bermuda. (a) *Oculina* from the marine facies of the Belmont Formation (~200 ka), Grape Bay (Fig. 8); (b) *Siderastrea* from the Devonshire marine member (~120 ka), Rocky Bay; (c) *Montastraea cavernosa* from the Devonshire marine member (~120 ka), Grape Bay; (d) *Diploria* from the Devonshire marine member (~120 ka), Coco Reef (Fig. 8). Knife for scale in (b) and (c) is 5.5 cm long; rock hammer in (d) is 0.3 m long. All photographs by D. R. Muhs.

values. As mentioned earlier, Thompson et al. (2003), using observations of trends noted earlier by Gallup et al. (1994), devised an open-system method of correcting ages that show high initial $^{234}U/^{238}U$ values. We recalculated the ages of the corals from both New Providence Island and Bermuda using this method (Table 1). Results indicate "open-system ages" ranging from ~127 to ~115 ka for New Providence Island and ~122 to ~111 ka for Bermuda. The results do not change our interpretation that the fossil corals on both islands correlate with the LIG or MIS 5.5.

5.2. U-series age estimates of oolite- and peloid-dominated marine and eolian sediments

As discussed in section 2, ooids and peloids have the potential for age determination by U-series dating. Building on the early findings of Thurber (1962), Broecker and Thurber (1965) and Osmond et al. (1965) showed that the Miami Limestone of Florida, which is composed largely of ooids, could be of LIG age, based on U-series dating. Interestingly, both of these early studies indicate a LIG age for this formation, even though the samples studied by Broecker and Thurber (1965) were 98% aragonite and those studied by Osmond et al. (1965) were less than 50% aragonite. Consistent with this observation, Muhs et al. (2011) reported similar LIG ages by TIMS U-series methods for the Miami Limestone, regardless of aragonite content of the bulk oolites.

Because of these approximate, but nevertheless promising results, we undertook U-series analyses of those beach and eolian sediments on New Providence Island that are dominated by U-bearing ooids and peloids. Sediments we collected that have a substantial skeletal component, based on thin section examination, were not utilized for dating. Beach sediments at various localities

(Fig. 3) and eolian sediments (mostly from the Lyford Cay section shown in Fig. 7) that were analyzed all have ooids and peloids as the dominant grains, but aragonite contents vary considerably, from ~30 to ~97% (Table 2). In doing these analyses, we have relaxed the closed-system requirement of U content equal to modern ooids and peloids, as the variable calcite contents will of course generate variable U contents through dilution. Nevertheless, most sediments analyzed have U contents fairly close to those of modern ooids and peloids, generally in the range of 2–4 ppm; those with less than 2 ppm have aragonite contents that are generally in the range of 32–47% (Table 2).

Results of these analyses show that the majority of oolitic/peloidal beach and eolian sediments of New Providence Island likely do correlate with the LIG (Table 2). One sample (NPI-87) shows evidence of a substantial open-system history, with much lower U content, and unsupported ^{230}Th. Most other samples analyzed show some evidence of open-system conditions, based on their positions on a $^{230}Th/^{238}U$ vs. $^{234}U/^{238}U$ isotopic evolution diagram (Fig. 12a). Nevertheless, on an isotope evolution diagram, the whole suite of samples shows a roughly linear array, similar to that from the Florida Keys (Fig. 12b), with an intersection near the ~125 ka isochron on the closed-system isotopic pathway. This observation suggests that the open-system correction method of Thompson et al. (2003) could be appropriate for the New Providence Island oolite/peloid sediments. Recalculation of these data using this method indicates a range (with two exceptions, NPI-70 [~134 ka] and NPI-86 [~105 ka]) of open-system ages from ~129 to ~114 ka, very similar to the range of open-system coral ages from both New Providence Island and Bermuda.

At the Lyford Cay section, the open-system ages derived from analyses there show that units "ii,", "iii", "iv," and "v" all contain

Table 1

U and Th concentrations, isotopic activity ratios, and ages of corals from New Providence Island, Bahamas and Bermuda.

Sample	Locality	Species	Growth-position?	Elevation (m)	Aragonite (%)	U ppm	+/−	232Th ppm	% error	230Th/232Th AR[a]	% error	234U/238U AR[a]	+/−	230Th/238U AR[a]	+/−	230Th/238U Age (ka)[b]	+/−	234U/238U initial AR[a]	+/−	Open-system 230Th/238U Age (ka)[c]	+/−
NEW PROVIDENCE ISLAND, BAHAMAS																					
NPI - 50 - C	Northwest Point	*Orbicella* sp., cf. *O. annularis*	Yes	2.4	96	2.64	0.13	0.0019	0.41	3217	0.43	1.1103	0.0018	0.7789	0.0033	**127.8**	**1.1**	**1.1582**	**0.0024**	123.2	1.6
NPI - 50 - E	Northwest Point	*Orbicella* sp., cf. *O. annularis*	Yes	2.4	98	2.71	0.11	0.0005	0.31	12,419	0.43	1.1144	0.0017	0.7834	0.0026	128.2	0.9	1.1643	0.0022	121.1	1.5
NPI - 50 - F	Northwest Point	*Orbicella* sp., cf. *O. annularis*	Yes	2.4	100	2.75	0.13	0.0007	0.42	9017	0.60	1.1139	0.0025	0.7745	0.0034	125.6	1.2	1.1623	0.0033	119.3	2.1
NPI - 50 - G- 1	Northwest Point	*Acropora cervicornis*	Yes	2.4	97	2.60	0.12	0.0325	0.45	194	0.54	1.1148	0.0024	0.7980	0.0038	132.6	1.3	1.1669	0.0032	nc	
NPI - 50 - H- 1	Northwest Point	*Acropora cervicornis*	Yes	2.4	100	2.89	0.12	0.0318	0.34	243	0.51	1.1159	0.0017	0.8800	0.0032	161.5	1.5	1.1829	0.0025	nc	
NPI - 400-P	Gambier	*Orbicella* sp., cf. *O. annularis*	Yes	3.8	95	2.54	0.12	0.0006	0.31	9312	0.37	1.1038	0.0018	0.7651	0.0026	**125.2**	**0.9**	**1.1478**	**0.0024**	124.9	1.6
NPI - 400-Q	Gambier	*Orbicella* sp., cf. *O. annularis*	Yes	3.8	99	2.71	0.11	0.0005	0.24	12,636	0.31	1.1103	0.0017	0.7461	0.0019	**118.3**	**0.6**	**1.1540**	**0.0022**	115.4	1.3
NPI - 400-R	Gambier	*Orbicella* sp., cf. *O. annularis*	Yes	3.8	96	2.58	0.11	0.0022	0.25	2691	0.26	1.1014	0.0019	0.7641	0.0021	**125.5**	**0.8**	**1.1446**	**0.0025**	126.6	1.7
NPI - 407-D	Winton	*Siderastrea* sp.	No	4.1	96	2.73	0.11	0.0007	0.33	9449	0.42	1.1047	0.0018	0.7436	0.0026	**118.8**	**0.8**	**1.1464**	**0.0023**	119.0	1.6
BERMUDA (this study)																					
CR-101	Coco Reef	*Diploria* sp.	Yes?	2.3	99	3.03	0.11	0.0009	0.33	7798	0.42	1.1118	0.0016	0.7309	0.0026	**113.8**	**0.8**	**1.1541**	**0.0020**	110.9	1.3
RB-101A	Rocky Bay	*Porites* sp.	Yes?	3	99	3.43	0.11	0.0051	0.55	1495	0.57	1.1013	0.0020	0.7339	0.0041	116.8	1.2	1.1409	0.0026	119.5	1.8
GB-17A	Grape Bay	*Diploria strigosa*	No	1.1 to 5.7	96	2.64	0.11	0.0003	0.32	19,727	0.42	1.1047	0.0015	0.7427	0.0025	**118.5**	**0.8**	**1.1463**	**0.0020**	118.8	1.3
GB-18	Grape Bay	*Diploria* sp. ?	Yes?	1.1 to 5.7	97	2.97	0.11	0.0011	0.40	5823	0.50	1.1084	0.0020	0.7415	0.0030	**117.4**	**0.9**	**1.1510**	**0.0026**	115.8	1.6
BERMUDA (ages recalculated from data in Muhs et al., 2002, with new half-lives from Cheng et al., 2013)																					
GB-2A	Grape Bay	*Siderastrea* sp.	No	1.1 to 5.7	98	3.08		0.0172		412		1.1101	0.0018	0.7572	0.0022	**121.4**	**0.8**	**1.1551**	**0.0024**	118.1	1.5
GB-6	Grape Bay	*Colophyllia* sp.	No	1.1 to 5.7	99	2.82	0.11	0.0012	0.40	5067	0.68	1.1073	0.0017	0.7389	0.0030	**116.9**	**0.9**	**1.1492**	**0.0022**	116.0	1.4
GB-7	Grape Bay	*Montastrea cavernosa*	No	1.1 to 5.7	99	2.75	0.12	0.0009	0.40	6834	0.90	1.1077	0.0021	0.7274	0.0030	**113.7**	**0.9**	**1.1484**	**0.0027**	113.1	1.7
GB-9	Grape Bay	*Siderastrea siderea*	No	1.1 to 5.7	100	3.02	0.11	0.0009	0.38	7982	2.03	1.1103	0.0017	0.7477	0.0029	**118.7**	**0.9**	**1.1542**	**0.0022**	115.8	1.4
GB-10	Grape Bay	*Colophyllia natans*	No	1.1 to 5.7	96	2.81	0.12	0.0020	0.22	3152	0.46	1.1073	0.0017	0.7471	0.0019	**119.2**	**0.6**	**1.1502**	**0.0022**	117.9	1.4
GB-11	Grape Bay	*Montastrea cavernosa*	No	1.1 to 5.7	99	2.75	0.11	0.0013	0.32	4851	0.34	1.1093	0.0013	0.7715	0.0026	**125.8**	**0.8**	**1.1559**	**0.0018**	122.2	1.2

[a] AR = isotopic activity ratio.

[b] Calculated using half lives of 75,584 yr for 230Th and 245,620 yr for 234U (Cheng et al., 2013); numbers in bold indicate those samples that are interpreted to have minimally biased age estimates.

[c] Calculated using open-system method of age correction from Thompson et al. (2003); "nc" indicates not calculated because of evidence of bulk U loss.
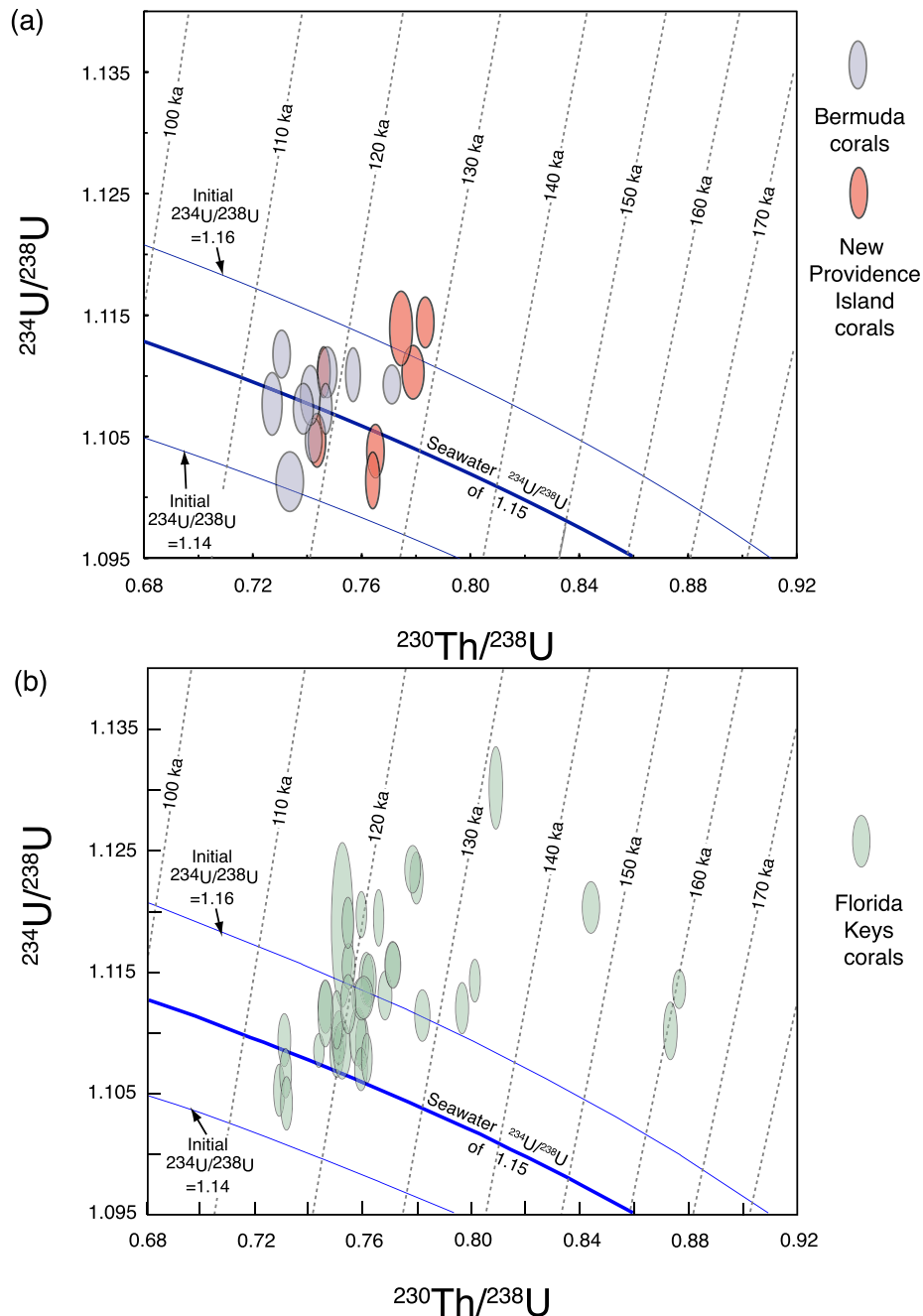
Fig. 11. Isotopic evolution diagrams for corals from (a) New Providence Island and Bermuda, with comparison to the Florida Keys (b). New Providence Island data and some Bermuda data are from the present study (Table 1); other Bermuda data are for corals from the Devonshire marine member at Grape Bay in Muhs et al. (2002), but do not include two samples that have evidence of U loss. Florida Keys data are from Muhs et al. (2011). Blue lines show isotopic evolution pathways for corals having closed-system history and initial $^{234}U/^{238}U$ activity values of 1.16, 1.15, and 1.14, which bracket measured values of modern seawater (Chen et al., 1986; Delanghe et al., 2002). Graphs constructed using ISOPLOT software of Ludwig (2001). (For interpretation of the references to color in this figure legend, the reader is referred to the Web version of this article.)

ooids and peloids that date to the LIG (Fig. 13). Unit "ii" beach sediments have ages of ~124 to ~119 ka and eolian sediments have ages of ~134 and ~118 ka. Unit "iii" beach sediments, sampled in two places, have ages of ~121 ka and eolian facies sediments of this unit have ages of ~123 and ~121 ka. These observations support the interpretation of Garrett and Gould (1984) that oolitic/peloidal beach sediments were the source of sands in the eolianite facies downwind, and were likely deposited at about the same time. It also appears that units "ii" and "iii" likely date to the same high-sea stand during the LIG. Based on stratigraphic position, the ooids and

peloids in eolianite units "iv" and "v" were likely deposited from beach sediments somewhat later, but apparently were also derived from beach sources of LIG age.

6. Estimates of sea level during the last interglacial period

6.1. New Providence Island

The patch reefs on New Providence Island provide our first estimate of LIG paleo-sea level. The patch reef at NPI-50 has a shore-

Table 2
U and Th concentrations, isotopic activity ratios, and ages of oolitic/peloidal beach and eolian deposits on New Providence Island, Bahamas.

Sample	Aragonite (%)	Lyford Cay unit	U ppm	+/−	^{232}Th ppm	% error	^{234}U/^{238}U AR[a]	+/−	^{230}Th/^{238}U AR[a]	+/−	^{230}Th/^{232}Th AR[a]	% error	^{230}Th/^{238}U Age (ka)[b]	+/−	^{234}U/^{238}U initial AR[b]	+/−	Open-system ^{230}Th/^{238}U Age (ka)[c]	+/−
NPI-66	45	Lyford Cay v	2.38	0.11	0.0088	0.31	1.1019	0.0020	0.7739	0.0026	635	0.40	**128.4**	**0.9**	**1.1464**	**0.0027**	128.6	1.8
NPI-65	57	Lyford Cay iv	3.78	0.11	0.0076	0.93	1.1140	0.0016	0.7768	0.0072	1169	0.97	126.3	2.2	1.1628	0.0023	119.8	2.1
NPI-65 dup #1	57	Lyford Cay iv	3.83	0.11	0.0074	0.36	1.1143	0.0018	0.7740	0.0029	1220	0.37	125.4	1.0	1.1628	0.0024	118.9	1.5
NPI-60	78	Lyford Cay iii	2.74	0.11	0.0121	0.33	1.1165	0.0018	0.7898	0.0028	543	0.48	129.6	1.0	1.1679	0.0024	121.0	1.6
NPI-61	65	Lyford Cay iii	3.03	0.11	0.0058	0.29	1.1186	0.0024	0.8056	0.0025	1269	0.47	134.0	1.0	1.1732	0.0032	123.2	2.0
NPI-64	40	Lyford Cay iii	2.41	0.11	0.0057	0.26	1.1259	0.0018	0.8217	0.0023	1049	0.40	137.2	0.9	1.1855	0.0024	121.5	1.5
NPI-18	97	Lyford Cay iii	4.59	0.14	0.0054	0.26	1.1131	0.0023	0.7790	0.0023	2002	0.27	127.2	0.9	1.1619	0.0031	121.0	1.9
NPI-18A	32	Lyford Cay iii	1.74	0.11	0.0027	0.36	1.1073	0.0022	0.7693	0.0029	1520	0.49	**125.7**	**1.0**	**1.1529**	**0.0030**	123.2	1.9
NPI-69	75	Lyford Cay ii	4.98	0.11	0.0121	0.21	1.1029	0.0013	0.7334	0.0018	918	0.37	**116.3**	**0.6**	**1.1429**	**0.0017**	118.1	1.1
NPI-70	40	Lyford Cay ii	2.40	0.11	0.0107	0.30	1.0826	0.0025	0.7305	0.0024	496	0.32	119.9	0.9	1.1158	0.0033	134.0	2.2
NPI-62	68	Lyford Cay ii	2.84	0.11	0.0090	0.72	1.1189	0.0022	0.8096	0.0059	778	0.75	135.2	2.0	1.1742	0.0031	124.0	2.3
NPI-62 dup #1	68	Lyford Cay ii	2.85	0.11	0.0092	0.37	1.1228	0.0016	0.8112	0.0031	761	0.44	134.7	1.1	1.1796	0.0022	121.3	1.5
NPI-19	98	Lyford Cay ii	3.95	0.13	0.0104	0.35	1.1205	0.0020	0.7960	0.0029	921	0.39	130.5	1.0	1.1742	0.0027	119.4	1.7
NPI-19A	47	Lyford Cay ii	1.74	0.12	0.0051	0.69	1.1244	0.0024	0.8178	0.0057	844	0.71	136.4	2.0	1.1828	0.0033	121.7	2.4
NPI-73	57	Blue Hill Rd	2.91	0.11	0.0057	0.40	1.1111	0.0016	0.7509	0.0031	1161	0.46	**119.5**	**1.0**	**1.1556**	**0.0021**	115.9	1.4
NPI-74	40	West of 73	2.91	0.12	0.0094	0.58	1.1335	0.0020	0.8405	0.0050	791	0.62	141.3	1.7	1.1989	0.0029	120.1	2.0
NPI-74 dup #1	40	West of 73	2.91	0.11	0.0096	0.29	1.1319	0.0019	0.8357	0.0026	767	0.42	140.2	1.0	1.1959	0.0026	120.2	1.6
NPI-75	65	East of 74	2.49	0.11	0.0103	0.41	1.1215	0.0022	0.7874	0.0034	579	0.53	127.7	1.1	1.1742	0.0030	116.6	1.9
NPI-76	50	West of 74	2.16	0.11	0.0050	0.45	1.1497	0.0025	0.9004	0.0042	1185	0.59	157.3	1.8	1.2334	0.0035	122.1	2.3
NPI-78	42	FrkWatsonRd	3.12	0.11	0.0050	0.25	1.0996	0.0015	0.7270	0.0020	1370	0.40	115.2	0.6	1.1378	0.0020	119.2	1.3
NPI-79	35	CarmichaelRd	3.82	0.11	0.0051	0.59	1.0763	0.0018	0.6232	0.0037	1407	0.73	93.0	0.9	1.0992	0.0023	113.7	1.5
NPI-79 dup #1	35	CarmichaelRd	3.81	0.11	0.0051	0.37	1.0779	0.0015	0.6280	0.0024	1417	0.46	93.9	0.6	1.1015	0.0019	113.5	1.2
NPI-80	35	CarmichaelRd	2.05	0.12	0.0057	0.32	1.1209	0.0019	0.7896	0.0027	860	0.36	128.5	0.9	1.1738	0.0025	117.6	1.6
NPI-81	33	CarmichaelRd	1.85	0.11	0.0050	0.40	1.1250	0.0021	0.8175	0.0034	908	0.42	136.1	1.2	1.1836	0.0029	121.1	1.9
NPI-83	44	Cowper Rd	2.04	0.11	0.0061	0.39	1.1349	0.0013	0.8526	0.0034	868	0.51	145.0	1.2	1.2032	0.0018	122.0	1.3
NPI-85	30	Cowper Rd	2.40	0.11	0.0038	0.35	1.1012	0.0020	0.7478	0.0027	1424	0.43	**120.8**	**0.9**	**1.1422**	**0.0026**	122.8	1.8
NPI-86	57	Clifton Pier	2.58	0.11	0.0085	0.38	1.1461	0.0018	0.8162	0.0032	753	0.49	130.4	1.0	1.2110	0.0025	105.1	1.5
NPI-87	57	Clifton Pier	1.91	0.11	0.0148	0.21	1.1831	0.0019	1.2651	0.0030	496	0.34	nc	nc	nc	nc	nc	nc

[a] AR = isotopic activity ratios; uncertainties are 2-sigma.

[b] Calculated with half-lives of 75,584 yr for ^{230}Th and 245,620 yr for ^{234}U (Cheng et al. (2013); numbers in bold indicate those samples that are interpreted to have minimally biased age estimates.

[c] Calculated using open-system method of age correction from Thompson et al. (2003); "nc" indicates not calculated.
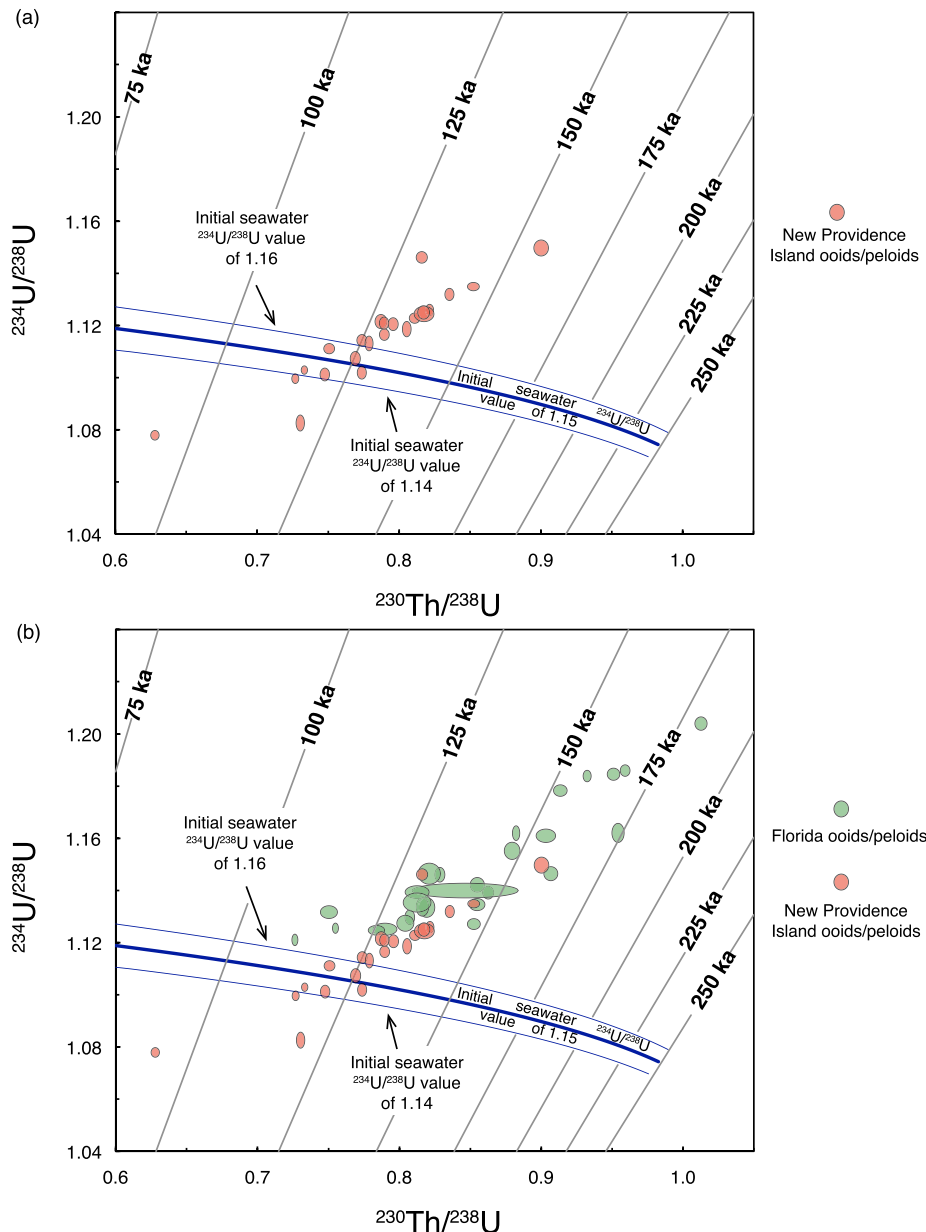
Fig. 12. Isotopic evolution diagrams for ooid and peloid samples from (a) New Providence Island, with comparison to ooid samples from the Florida Keys and the Miami, Florida area (b). New Providence Island data are from the present study (Table 2); Florida data are from Muhs et al. (2011). Blue lines show isotopic evolution pathways for corals having closed-system history and initial ^{234}U/^{238}U activity values of 1.16, 1.15, and 1.14, which bracket measured values of modern seawater (Chen et al., 1986; Delanghe et al., 2002). Note rough linear trend of ellipses, with intersection within closed-system range at ~125 ka. Graphs constructed using ISOPLOT software of Ludwig (2001). (For interpretation of the references to color in this figure legend, the reader is referred to the Web version of this article.)

normal extent of ~10 m, an outer edge at ~1 m above sea level, and a maximum elevation of 2.4 m (by GPS) or 3.0 m (by topographic map). A reddish-brown soil has formed on this reef; 10 m inland, the reef is covered by a skeletal eolianite that we hypothesize to be of Holocene age. Colonies of *Acropora cervicornis*, *Diploria* sp., and *Orbicella* sp. are present in this patch reef, many in growth position. Based on observations reported by Goreau (1959) and Goreau and Goreau (1973) in Jamaica, Shinn et al. (1989) in the Florida Keys, and Hibbert et al. (2016) for other Caribbean/western Atlantic localities, some of these corals have considerable depth ranges. *Acropora cervicornis*, for example, has optimum habitat depths of 15–30 m in the Florida Keys, but is found as deep as 50 m; on Jamaica, modern colonies of this taxon are typically found in the "mixed zone" from 7 to 15 m depth. Common species of *Diploria* sp.

have optimum depths of 1–15 m around the Florida Keys at present, but can be found as deep as 25–40 m. The most common species of *Orbicella*, *O. annularis*, has optimum habitat depths of 3–45 m, but this taxon can be found at depths of up to ~80 m. Thus, there is a considerable range of options for estimating paleo-sea level based on the measured elevation of these colonies and their possible depths at the time of growth. We have taken a conservative approach and added only 3 m as a *minimum*, optimal habitat depth requirement to our paleo-sea level estimates for this patch reef. This would indicate a possible LIG paleo-sea level of 5.4–6.0 m for the NPI-50 patch reef, but we stress that this estimate could be considerably higher. The other patch reef, NPI-400 (Fig. 3) is west of NPI-50, but also has a shore-normal extent of ~10 m, an outer edge ~1.75 m above sea level, and a maximum elevation of ~3.8 m (by
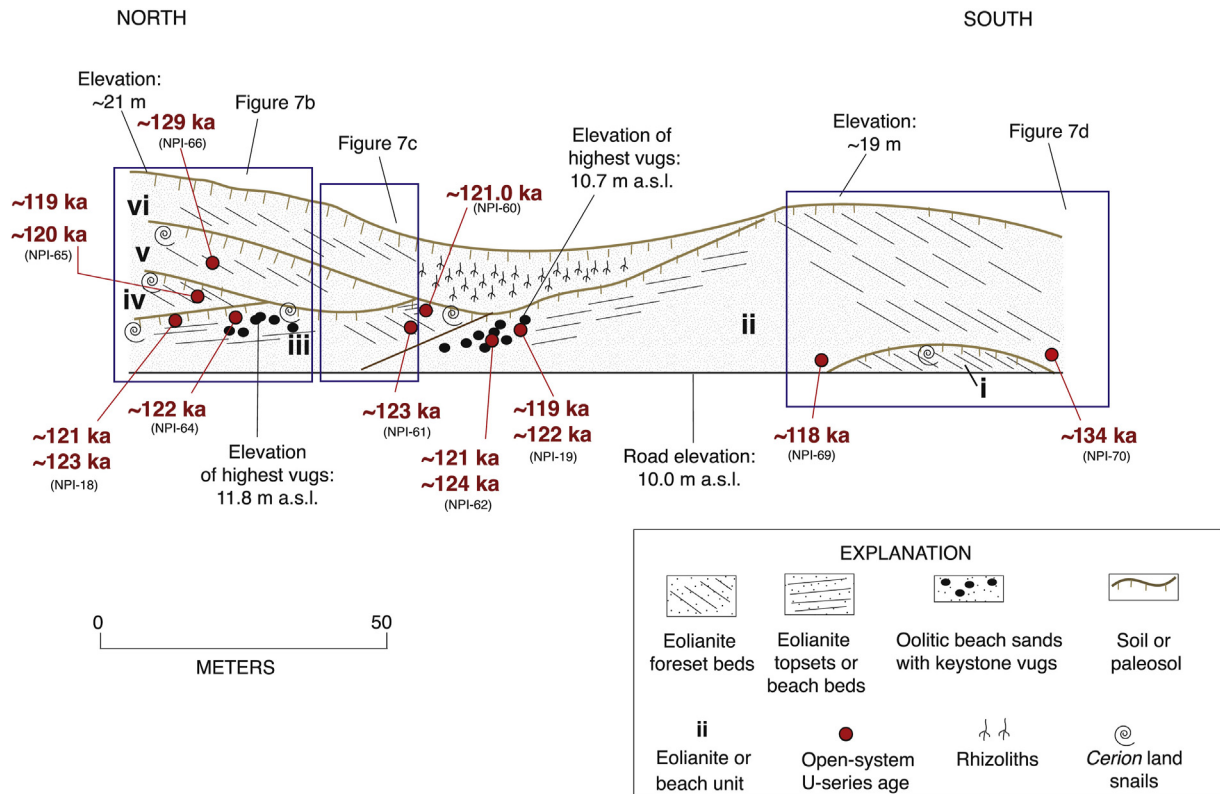
Fig. 13. Stratigraphy of beach and eolianite deposits and GPS-derived beach elevations at Lyford Cay, New Providence Island (Fig. 3), redrawn in slightly modified form from Garrett and Gould (1984). Filled red circles are open-system U-series ages of ooid-peloid-dominated sediments (from Table 2), using correction method of Thompson et al. (2003). (For interpretation of the references to color in this figure legend, the reader is referred to the Web version of this article.)

both GPS and topographic map). A patchy reddish-brown, clay-rich soil is found on the top of the emergent reef, and horizontal beds of carbonate sand extend landward and slightly above the reef for about 6 m. Like NPI-50, colonies of *Acropora cervicornis*, *Diploria* sp., and *Orbicella* sp. in growth position are present in this reef. Once again taking our conservative adjustment of ~3 m for depth habitat, we can estimate a *minimum* LIG paleo-sea level of ~6.8 m for the patch reef at NPI-400. Alternatively, based on the observations of Goreau (1959) and Goreau and Goreau (1973) for *Acropora cervicornis* colonies, we could instead assume a habitat depth of ~7 m, making paleo-sea level estimates as high as ~9 m for NPI-50 and ~10 m for NPI-400.

If we are correct in our interpretation that the oolitic/peloid beach facies sediments in much of southern and western New Providence Island date to the last interglacial period, it is possible to use the elevations of vugs, or beach fenestrae, as paleo-sea level indicators. The use of vugs as paleo-sea level indicators is supported by two other lines of evidence. One is that vugs we observed are found within sediments whose beds dip gently (~3° to ~8°) seaward, typical of beach face sediments. The other line of reasoning is that most of these localities, as pointed out by Garrett and Gould (1984), are topographically higher than the surrounding terrain and can be traced laterally in a shore-parallel direction (Fig. 3), providing geomorphic support for their interpretation as beach ridges.

With the exception of the possibly younger (open-system age of ~105 ka) locality near Clifton Pier (NPI-86), beach ridge elevations range from 4.0 to 14.3 m, with most elevations falling between 5.0 and 9.6 m (Table 3 and Fig. 14). The highest elevations are in the western part of the island, at locality NPI-78 and at Lyford Cay

(Fig. 3), where elevations of 14.3 and 11.8 m (for unit "iii"), respectively, were measured. Our elevation data are in reasonable agreement with those of Garrett and Gould (1984; their Fig. 11). It should be noted that these investigators corrected their field elevation measurements for an assumed long-term subsidence of the Bahama Banks of ~3 m per 125 ka. Recalculating their reported measurements without this "correction" yields a range of elevation values of 13.0 m (at Lyford Cay) to 6.6 m (a short distance southeast of our coral-bearing sediment locality NPI-407), with most of their beach ridge elevations falling between 8.0 and 11.8 m, in broad agreement with those of the present study. The question of how paleo-sea level estimates, from both patch reefs and beach vugs, could be affected by long-term subsidence is an important one, and is addressed in later discussion.

6.2. Bermuda

On Bermuda, estimates of paleo-sea level are more difficult to make, because precise sea-level indicators, such as vugs or growth-position corals, are lacking or rare within the Devonshire marine member of LIG age. Rarely, there are fossil occurrences of accretionary lips of algal-vermetid growth that mark approximate low-tide level, and Meischner et al. (1995) report one such feature of LIG age at Watch Hill Park (Fig. 8) at an elevation of ~5.8 m. Elsewhere, many of the exposures of Devonshire marine sediments consist of fossiliferous sand and gravel deposited on wave-cut benches or notches eroded into older units, particularly the Belmont Formation. As such, they provide at least minimum-limiting elevations for paleo-sea level during the LIG. At two localities, Rocky Bay and Coco Reef, we found *Siderastrea* and *Diploria* colonies

Table 3
Composition, elevation, and coordinates of patch reefs and oolitic/peloidal sediments on New Providence Island.

Sample	Aragonite (%)	Location	Lyford Cay unit	Facies	Notes	Composition*	Longitude (°)	Latitude (°)	Reef or beach vug elevation, meters GPS (topo)
NPI-50	See Table 1	Northwest Point	n/a	patch reef			−77.495991735	25.062575286	2.4 (3.0)
NPI-400	See Table 1	Gambier area	n/a	patch reef			−77.469360580	25.065649990	3.8 (3.7)
NPI-407	See Table 1	Winton area	n/a	beach with corals			−77.264055570	25.044826325	4.1
NPI-66	45	Lyford Cay	v	eolian	foresets	O=P ≫ S	−77.531725000	25.023078000	n/a
NPI-65	57	Lyford Cay	iv	eolian	above paleosol	O > P > S	−77.531725000	25.023078000	n/a
NPI-60	78	Lyford Cay	iii	eolian	topsets	O > P ≫ S	−77.532034349	25.022690376	n/a
NPI-61	65	Lyford Cay	iii	eolian	foresets	O > P > S	−77.532034349	25.022690376	n/a
NPI-64	40	Lyford Cay	iii	beach	vug-bearing	O > P ≫ S	−77.531725000	25.023078000	11.8
NPI-18	97	Lyford Cay	iii	beach	vug-bearing	O > P ≫ S	−77.531725000	25.023078000	11.8
NPI-18A	32	Lyford Cay	iii	beach	vug-bearing	O > P ≫ S	−77.531725000	25.023078000	11.8
NPI-69	75	Lyford Cay	ii	eolian	foresets north of unit i	O > P ≫ S	−77.532490000	25.021940000	n/a
NPI-70	40	Lyford Cay	ii	eolian	foresets south of unit i	O > P ≫ S	−77.532790000	25.021670000	n/a
NPI-62	68	Lyford Cay	ii	beach	vug-bearing	O > P	−77.532034349	25.022690376	10.7
NPI-19	98	Lyford Cay	ii	beach	vug-bearing	O + P ≫ S	−77.532034349	25.022690376	10.7
NPI-19A	47	Lyford Cay	ii	beach	vug-bearing	O + P ≫ S	−77.532034349	25.022690376	10.7
NPI-73	57	Blue Hill Rd	n/a	beach	vug-bearing	O > P ≫ S	−77.353847286	25.018217787	9.6 (9.7)
NPI-74	40	West of 73	n/a	beach	vug-bearing	O > P	−77.363204133	25.015145434	7.4 (7.9)
NPI-75	65	East of 74	n/a	beach	vug-bearing	O > P	−77.362355352	25.015409660	7.4 (7.9)
NPI-76	50	West of 74	n/a	beach	vug-bearing	O=P ≫ S	−77.372970843	25.013865010	6.4 (7.3)
NPI-78	42	Frank Watson Rd	n/a	beach	vug-bearing	O > P	−77.517868843	25.015679452	14.3 (14.6)
NPI-79	35	Carmichael Rd	n/a	beach	vug-bearing	O ≫ P	−77.481435240	25.006578230	4.9 (6.7)
NPI-80	35	Carmichael Rd	n/a	beach	vug-bearing	O ≫ P	−77.445893106	25.002236438	5.8 (5.0)
NPI-81	33	Carmichael Rd	n/a	beach	vug-bearing	O > P ≫ S	−77.415466859	25.005452129	8.9 (7.6)
NPI-83	44	Cowper Rd	n/a	beach	vug-bearing	O > P	−77.397756939	25.003874653	8.2
NPI-85	30	Cowper Rd	n/a	eolian	foresets	O > P ≫ S	−77.416250495	25.005459529	n/a
NPI-86	57	Clifton Pier	n/a	beach, upper	vug-bearing	O ≫ P	−77.536376879	25.001739962	4.1
NPI-87	57	Clifton Pier	n/a	beach, lower	vug-bearing	O > P > S	−77.536376879	25.001739962	2.8

*O = ooids; P = peloids; S = skeletal fragments.

that appear to be in growth position (Fig. 10b, d) and a *Diploria* colony at Grape Bay may also be in growth position. The elevations of these fossils, along with consideration of their minimum optimal depth requirements of ~3 m (Shinn et al., 1989; see also Hibbert et al., 2016), also provide minimum-limiting paleo-sea levels.

Overall, we utilized paleo-sea level elevation data from three sources for Bermuda. The first source includes the three localities (Coco Reef, Rocky Bay, and Grape Bay) where we have U-series ages on growth-position corals and elevation measurements, all from the present study, as described earlier. The second source is localities that are undated, but have been mapped as Devonshire marine deposits based on sedimentology and stratigraphic position, and where elevations were measured by us (Fort Scaur, Boaz Island, Ireland Island South, Long Island, Verrill Island, Bailey's Bay, and Whalebone Bay). Finally, the third source includes localities where Harmon et al. (1983) reported LIG U-series ages of corals and elevation measurements (Sugar Cane Point, Hawkins Island, Saucos Hill, Watch Hill Park, Coney Island, and Cable Bay Point). At a number of localities, we measured elevations reported by Harmon et al. (1983) and our measurements agree with theirs.

Results for Bermuda show a narrow range of LIG elevations, from ~2 m or slightly less (Sugar Cane Point, Long Island, Bailey's Bay, and Coney Island) to 5–8 m (Boaz Island, Ireland Island South, Hawkins Island, Coco Reef, Grape Bay, Rocky Bay, and Watch Hill Park). Measurements at Coco Reef and Rocky Bay are based on elevations of what appear to be growth-position corals, with a minimum habitat depth correction of ~3 m, yielding minimum-limiting LIG paleo-sea level estimates of ~5.3 and ~6 m, respectively (Fig. 15). At Watch Hill Park, marine deposits containing corals occur at 3 m above sea level (Harmon et al., 1983), but an algal-vermetid lip, considered to be of LIG age, is found above these deposits, at 5.8 m above sea level (Meischner et al., 1995). Overall, elevations are lower than those on New Providence Island, but many of the Bermudan elevation measurements could be minimum values.

7. Discussion

7.1. Ages of marine deposits on New Providence Island and Bermuda

There have been a number of studies of LIG marine deposits on islands of the western Atlantic and Caribbean. Previous high-precision U-series ages of corals from LIG deposits on the Bahamas have been generated mainly from San Salvador Island (Fig. 2) and Great Inagua Island (~300 km south of San Salvador Island). Chen et al. (1991) reported the first suite of high-precision ages for these islands, but Thompson et al. (2011) provided a more extensive set of ages. In addition, Thompson et al. (2011) applied the open-system correction method of Thompson et al. (2003) to their Bahamas corals, yielding an age range of ~126 to ~111 ka.

From elsewhere in the western Atlantic and Caribbean we have analyzed LIG corals from emergent marine deposits and applied the Thompson et al. (2003) correction method. Open-system ages generated in this manner yield age ranges of ~128 to ~110 ka for Barbados and ~132 to ~111 ka for southern Cuba (Muhs and Simmons, 2017; Muhs et al., 2017). Using data from the Florida Keys reported by Muhs et al. (2011), we calculated open-system ages using the new half-lives of Cheng et al. (2013) and the open-system method of Thompson et al. (2003). Results indicate an age range for the Florida Keys of ~132 to ~111 ka (n = 38), with two outliers at ~147 and ~149 ka. Thus, the ranges of ages for the Bahamas, Barbados, Florida, and Cuba are in good agreement with one another and capture the generally accepted age range for the last interglacial period used by the sea-level modeling community (Dutton and Lambeck, 2012; Lambeck et al., 2012; Creveling et al., 2015, 2017; Dutton et al., 2015a; Dendy et al., 2017).

In the present study, open-system ages of corals and oolitic/peloidal sediments from New Providence Island and Bermuda are in good agreement with previous ages of the LIG from the region. Open-system ages of corals for New Providence Island range from

Table 4
Localities on Bermuda of last-interglacial (Devonshire marine member, ~120 ka) age and measured elevations above modern mean sea level.

Locality	Latitude (°N)	Longitude (°W)	Method of age estimate[a]	Reported age (ka) ± 2 sigma[b]	Open-system age (ka)[c]	Elevation (m)[d]	Age reference	Elevation reference
Fort Scaur	32.28548	64.87043	Stratigraphic position	Devonshire	N/A	4.0	Vacher et al. (1989)	This study
Sugar Cane Point	32.30525	64.86037	U-series, alpha spectrometry	118 ± 12	~128	2.1	Harmon et al. (1983)	This study
Boaz Island	32.31070	64.85253	Stratigraphic position	Devonshire	N/A	6.3	Vacher et al. (1989)	This study
Ireland Island South	32.31503	64.84685	Stratigraphic position	Devonshire	N/A	7.4	Vacher et al. (1989)	This study
Ireland Island South	32.31355	64.84208	Stratigraphic position	Devonshire	N/A	4.6	Vacher et al. (1989)	This study
Hawkins Island	32.28434	64.82912	U-series, alpha spectrometry	134 ± 16	~122	6	Harmon et al. (1983)	Harmon et al. (1983)
Long Island	32.28772	64.81538	Stratigraphic position	Devonshire	N/A	2.0	Vacher et al. (1989)	This study
Verrill Island	32.28995	64.81347	Stratigraphic position	Devonshire	N/A	5.75	Vacher et al. (1989)	This study
Coco Reef	32.27600	64.77267	U-series, TIMS	113.8 ± 0.8	~114	2.3	This study	This study
Grape Bay	32.28507	64.76427	U-series, TIMS	113.7 ± 0.9 to 125.8 ± 0.8	~113 to ~125	5.7	This study	This study
Rocky Bay	32.29762	64.74597	U-series, TIMS	116.8 ± 1.2	~117	3.0	This study	This study
Saucos Hill	32.30676	64.73346	U-series, alpha spectrometry	121 ± 12	~124 to ~130	4	Harmon et al. (1983)	Harmon et al. (1983)
Bailey's Bay	32.35042	64.72260	Stratigraphic position	Devonshire	N/A	1.6	Vacher et al. (1989)	This study
Watch Hill Park	32.31480	64.71705	U-series, alpha spectrometry	127 ± 12	~123	5.8	Harmon et al. (1983)	Meischner et al. (1995)
Coney Island	32.35952	64.71495	U-series, alpha spectrometry	124 ± 16	~120	1.0	Harmon et al. (1983)	This study
Whalebone Bay	32.36537	64.71383	Stratigraphic position	Devonshire	N/A	2.5	Vacher et al. (1989)	This study
Cable Bay Point	32.33454	64.68731	U-series, alpha spectrometry	124 ± 24	~126	4	Harmon et al. (1983)	Harmon et al. (1983)

[a] TIMS = thermal ionization mass spectrometry.

[b] Ages listed are given as reported in Harmon et al. (1983) and the present study (Table 1), except age uncertainties from Harmon et al. (1983) are given a 2-sigma uncertainty here. Undated localities are all mapped as belonging to the Devonshire Marine Member of the Rocky Bay Formation (Vacher et al., 1989), the same as for dated localities, but correlation of these localities to the Devonshire Marine Member is based on stratigraphic position.

[c] Open-system ages calculated by the authors from data in Table 1 (this study) and Harmon et al. (1983) using half-lives of Cheng et al. (2013) and method of Thompson et al. (2003).

[d] All elevations measured in the present study are corrected for tidal variations; coordinates and elevations reported by Harmon et al. (1983) are considered approximate.

~127 to ~115 ka. For ooid/peloid sediments from New Providence Island, open-system ages range from ~129 to ~114 ka, with two outliers at ~134 and ~105 ka. Combining the new U-series data from Bermuda with recalculated open-system ages from Bermudan data in Muhs et al. (2002) yields a range of open-system ages from ~122 to ~111 ka. All these age ranges are in good agreement with previous estimates of LIG reefs elsewhere in the Caribbean and western Atlantic.

7.2. The concept of a "dual peak" of high-sea levels during the LIG

For more than four decades, dating back to early studies on the Huon Peninsula of New Guinea (Bloom et al., 1974; Chappell, 1974), investigators have explored the idea that there were two discrete high stands of sea during the LIG. On New Guinea, reef complexes VIIa (a fringing reef) and VIIb (a barrier reef found in a seaward direction) have been interpreted as possibly reflecting two separate high-sea stands during this interglacial period. Precise U-series analyses of corals from these two reefs demonstrated that reef VIIb is almost certainly of LIG age (Stein et al., 1993). Although many of the reef VIIa corals showed open-system conditions (Stein et al., 1993), these data provided evidence that reef VIIa could date to the LIG as well. Both reefs are found at high elevations in this tectonically active region. Thus, it also could be argued that separate co-seismic uplift events during a single interglacial period could generate two or more emergent reefs. In support of this explanation, Ota et al. (1993) documented as many as six emergent

reef terraces of Holocene age on the Huon Peninsula, all uplifted during the present interglacial.

Following from the early New Guinea work, a study of emergent reefs on Atauro Island by Chappell and Veeh (1978) also suggested the possibility of a dual sea-level peak during the LIG. Chappell and Veeh (1978) used, as supporting evidence, the ages of lower, growth-position corals vs. the ages of overlying, detrital coral gravels from the Waimanalo Formation of Oahu, Hawaii. The ages these investigators used in this analysis were alpha-spectrometric U-series analyses presented by Ku et al. (1974). Newer, high-precision U-series ages from Oahu show no significant difference in the range of coral ages from these two facies (see Muhs et al., 2002, p. 1336).

On the island of Barbados, the Quaternary uplift rate is much lower than that on New Guinea, but more than one high stand of sea during the LIG has been proposed here too (Schellmann and Radtke, 2004; Thompson and Goldstein, 2005). On Barbados, however, no multiple Holocene terraces have been reported and co-seismic uplift is a less likely explanation for possible multiple LIG terraces. Based on detailed studies of internal reef architecture, Speed and Cheng (2004, p. 229) felt that sea-level excursions within the LIG, while possible, could not be resolved in the stratigraphic record on Barbados.

Multiple sea stands during the LIG from have been proposed from deep-sea records and reefs on tectonically stable coastlines. For example, Rohling et al. (2008), studying the oxygen isotope record in planktonic foraminifera recovered from Red Sea sediment
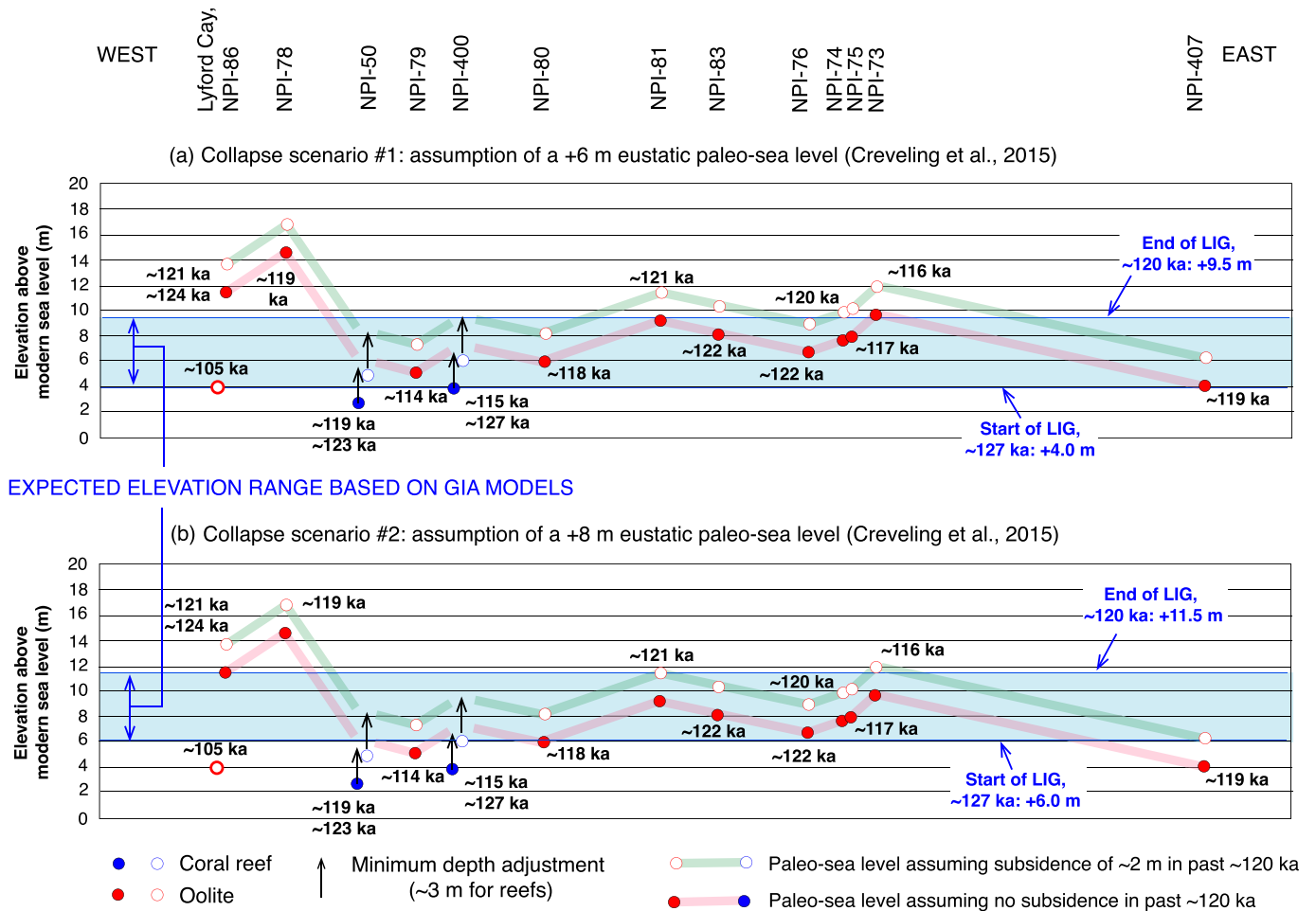
Fig. 14. Shore-parallel profiles, showing elevations of vug-bearing beach ridge sediments (filled red circles) and patch reefs (filled blue circles) on New Providence Island, Bahamas, all measured in the present study, connected by pink lines. Locality numbers are keyed to Fig. 3; see Table 3 for additional details. Numbers in bold are open-system U-series ages (Tables 1 and 2), using correction method of Thompson et al. (2003). Arrows on patch reef symbols indicate minimum corrections, assuming that reefs grew in at least 3 m of water, based on the present *optimal* habitat depths of coral taxa identified (Shinn et al., 1989; see also Hibbert et al., 2016). Blue shade in (a) represents GIA-modeled range of sea level at the beginning (~127 ka) and end (~120 ka) of the last-interglacial (LIG) high-sea stand, assuming a +6 m eustatic paleo-sea level ("collapse scenario #1" of Creveling et al., 2015). Panel (b) is the same as in (a) except the range of the last-interglacial (LIG) high-sea stand assumes a +8 m eustatic paleo-sea level ("collapse scenario #2" of Creveling et al., 2015). Also shown in both (a) and (b), with open circles, are paleo-sea level estimates based on measured elevations as described above, but with adjustment of long-term subsidence of ~2 m in the past ~120 ka (see text for discussion). (For interpretation of the references to color in this figure legend, the reader is referred to the Web version of this article.)

cores, suggested that there could have been as many as four separate high stands of sea during the LIG, between ~124 and ~117 ka, with a negative sea-level excursion of more than 10 m recorded between ~122 and ~120 ka, followed by a rise to sea level above present between ~120 and ~119 ka. As mentioned earlier, Thompson et al. (2011) provided new, high-precision U-series ages of corals from San Salvador Island and Great Inagua Island in the Bahamas (Fig. 2). Following on earlier studies by White et al. (1998) and Wilson et al. (1998), Thompson et al. (2011) proposed at least two high stands within the LIG and allowed for the possibility of as many as four high stands, comparing their data to the Red Sea record of Rohling et al. (2008). Skrivanek et al. (2018) reexamined the San Salvador and Great Inagua sites studied by White et al. (1998), Wilson et al. (1998), and Thompson et al. (2011) and concluded that there was evidence for a sea-level lowering of ~1 m within the LIG, possibly over a time period of a thousand years.

Modeling efforts have also addressed the question of a dual high-sea stand during the LIG. Kopp et al. (2009) conducted a statistical analysis of a database generated from many reported LIG deposits worldwide, from both tectonically active and stable coastlines. These investigators concluded that early within the LIG

there was a sea-level high, followed by a drop of ~4 m, succeeded by another sea-level high. Unfortunately, some of the hypothesized LIG sites used by Kopp et al. (2009) are either poorly dated or not dated at all. A subsequent study by these investigators provided a suite of options in model reconstructions of LIG sea level, with some including the Red Sea record of Rohling et al. (2008), others without it, and using a much more selective set of LIG sites that are confidently dated (Kopp et al., 2013). Their results still show two sea-level peaks during the LIG under all compilations, although the amplitudes differ from case to case (see Kopp et al., 2013, their Figure S-2).

If two or more high stands of sea occurred during the LIG were global phenomena, then in principle such a record could be found on New Providence Island. The Kopp et al. (2009) study proposed that sea level during the LIG peaked at ~124 ka, began to fall after that, reached a low point at ~120 ka, and rose again to a peak at ~118 ka. The Thompson et al. (2011) study, from elsewhere on the Bahamas, has a similar timing, proposing LIG sea level at +4 m at ~123 ka, +6 m at ~119 ka, and near present at some time in between. On NPI, corals in growth position are found in the two patch reefs we studied, at NPI-50 and NPI-400, only ~2.7 km apart from
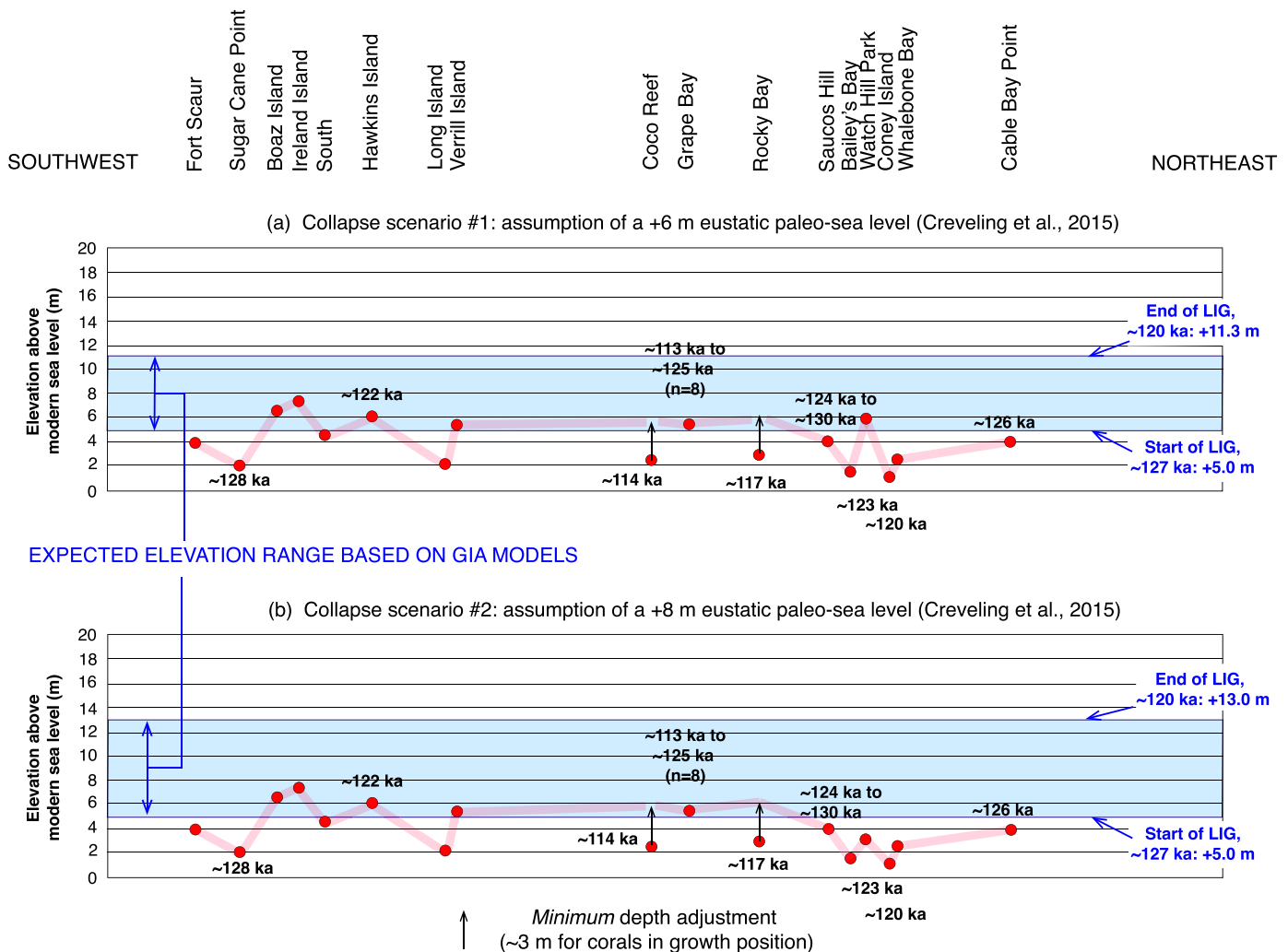
Fig. 15. Shore-parallel profiles, showing measured elevations of marine sediments of the Devonshire marine member of the Rocky Bay Formation, Bermuda, all measured in the present study, Harmon et al. (1983), or Meischner et al. (1995). Locality names are keyed to Fig. 8; see Table 4 for additional details. Numbers in bold are open-system U-series ages of corals (Table 1), using half-lives of Cheng et al. (2013) and correction method of Thompson et al. (2003) for localities at Coco Reef, Rocky Bay, and Grape Bay from this study and Muhs et al. (2002); other ages are from data reported by Harmon et al. (1983), recalculated in this study using half-lives of Cheng et al. (2013) and correction method of Thompson et al. (2003). Localities without U-series ages are those mapped as the Devonshire marine member by Vacher et al. (1989) based on stratigraphic position and sedimentology. Blue shade in (a) represents GIA-modeled range of sea level at the beginning (~127 ka) and end (~120 ka) of the last-interglacial (LIG) high-sea stand, assuming a +6 m eustatic paleo-sea level ("collapse scenario #1" of Creveling et al., 2015). Panel (b) is the same as in (a) except the range of the last-interglacial (LIG) high-sea stand assumes a +8 m eustatic paleo-sea level ("collapse scenario #2" of Creveling et al., 2015). (For interpretation of the references to color in this figure legend, the reader is referred to the Web version of this article.)

one another (Fig. 3). Using the same open-system method of age correction that Thompson et al. (2011) used in their Bahamas study, ages of growth-position corals from these patch reefs on NPI are ~127, ~125, ~123, ~121, ~119, and ~115 ka (Table 1). Thus, these coral colonies have ages that span the entire range of hypothesized sea-level rise, fall, and second rise in the proposed dual-peak LIG scenario, yet all occur close to one another, have little or no difference in elevation, and display no stratigraphic evidence of more than one period of patch reef development.

Garrett and Gould (1984) mapped multiple beach ridges on NPI (Fig. 3), all placed within their "Phase II" age group of LIG age. In principle, it could be argued that these multiple beach ridges on NPI could contain a record of more than one high-sea stand during the LIG. It is difficult, however, to interpret multiple beach ridges as indicative of multiple high stands of sea, separated by substantial regressions (see discussion in Murray-Wallace and Woodroffe, 2014). Multiple beach ridges can develop within a single high stand of sea with the higher-elevation landforms produced by storm waves and lower-elevation ridges formed by average waves.

Multiple beach ridges can also develop simply by progradation (assuming a sufficient sediment source) with a more-or-less continuous sea-level rise (see Oliver et al., 2020, for a Holocene example from Australia). On New Providence Island, at the Lyford Cay locality, the "unit ii" and "unit iii" beach deposits could be interpreted as two separate high-sea stands during the LIG (Fig. 13). The U-series ages of ooids and peloids from these two units show no significant differences, however, although we caution that those ages date the particles, not the times of formation of the ridges.

We conclude from these observations that NPI has no persuasive coral reef or beach ridge evidence supporting the dual-peak model for sea level within the LIG. Other islands that we have studied, such as tectonically stable Bermuda and the Florida Keys, and the slowly uplifting coasts of Curaçao and southern Cuba (Muhs et al., 2002, 2011, Muhs et al., 2012c, 2017), also offer no geomorphic, stratigraphic, or geochronologic evidence of more than one high-sea stand within the last interglacial period. Other researchers have challenged the dual-peak LIG sea-level history. Barlow et al. (2018), for example, point out that if the Kopp et al. (2009) model

is correct, such a scenario would require growth of 1.15−3.45 million km^3 of glacial ice in less than ~1000 yr. The same requirement would apply to the reconstruction presented by Rohling et al. (2008). For comparison, the contemporary inland ice sheet of Greenland is ~2.6 million km^3 (Weidick, 1995). If such a sea level drop had actually occurred within the LIG, it would be significant, because it would have required substantial ice sheet growth, possibly equivalent to that found now on Greenland, during a time when summer insolation in the Northern Hemisphere was high (Otto-Bliesner et al., 2006; Overpeck et al., 2006).

7.3. Estimating LIG sea level

As discussed earlier, testing the hypotheses of GIA effects on the geologic record of high sea levels on coastlines requires that several conditions be met. One is that a coast must be distant from plate boundaries and therefore tectonically stable. In the western Atlantic and Caribbean region, this eliminates islands such as Cuba, Hispaniola (Haiti and Dominican Republic), Barbados, and Curaçao, where tectonic activity is expected, given the geologic setting (Fig. 1), and long-term uplift has been documented in previous studies. North of the North American-Caribbean plate boundary, however, tectonic stability can be more reasonably assumed for localities such as the Yucatan peninsula, the Florida Keys, Florida mainland, the Bahamas, and Bermuda.

A second requirement is that reliable paleo-sea level indicators dating to the geologic time period of interest must be present. One of the best such indicators is the shoreline angle of erosional marine terraces on high-wave-energy coastlines, which is within a meter or two of mean sea level. Although such landforms are the norm on coastlines such as California (e.g., Muhs et al., 2012b), they are less common in the Caribbean and western Atlantic, although some authors have reported such features (see, for example, Speed and Cheng, 2004, for Barbados). Constructional reef terraces are much more common in the Caribbean and western Atlantic, but only certain corals that provide the frameworks for these reefs have depth habitats that constrain paleo-sea level closely. The best of these is *Acropora palmata*, which typically lives within the upper ~6 m of the water column (Goreau, 1959; Goreau and Goreau, 1973; Shinn et al., 1989; Hibbert et al., 2016). Although this taxon is commonly reported in emergent LIG reefs of the southern Bahamas, Barbados, and Curaçao, it is uncommon in the northern Bahamas, extremely rare in the Florida Keys (Stanley, 1966; Muhs et al., 2011), and to our knowledge has never been reported from Bermuda. Other coral species are less well constrained with respect to paleo-sea level estimates, even when well preserved and in growth position. Among these are taxa such as *Orbicella annularis*, *Montastraea cavernosa*, *Siderastrea*, *Diploria*, and *Colpophyllia*, all of which are more common in the northern Bahamas, Florida, and Bermuda. Based on observations reported by Goreau (1959), Goreau and Goreau (1973), Shinn et al. (1989), and Hibbert et al. (2016), some of these corals have considerable depth ranges, as noted earlier. Among a range of possible choices, we have added a conservative 3 m as a *minimum*, optimal habitat depth requirement to our paleo-sea level estimates for patch reefs on New Providence Island (that host *Orbicella* and *Diploria* in growth position) and for growth-position corals on Bermuda (*Diploria* and *Siderastrea*). We emphasize, therefore, that our estimates of paleo-sea level based on the depth-habitat-corrected elevations of these taxa are strictly minimum-limiting values.

Finally, another consideration for paleo-sea level estimates, even on tectonically stable islands, is long-term subsidence, whether due to sea floor spreading, sediment loading, or both of these processes. Garrett and Gould (1984), using data from Lynts (1970), used a long-term subsidence rate of Andros Island (Fig. 2)

to infer ~3 m of subsidence on New Providence Island since the LIG. Subsidence histories of both Andros Island and the Florida Keys, however, as illustrated in Lynts (1970) show decreasing values in the time from the Cretaceous to present. For New Providence Island and the Florida Keys, rather than use a long-term rate of subsidence since the Cretaceous, we chose to interpolate the Lynts (1970) curves for the time period since the beginning of the Oligocene, when rates of subsidence seemed to have diminished considerably. Thus, on Andros Island, there appears to have been ~680 m of subsidence in ~37.5 Ma, or a rate of ~0.018 m/ka. This long-term rate is consistent with a much shorter (~4.0 Ma), but higher-resolution subsidence record from San Salvador Island (Fig. 2) reported by McNeill et al. (1988). Using the longer-term record of Lynts (1970) for Andros Island, we estimate ~2.16 m of subsidence in the past ~120 ka. For New Providence Island, if we assume ~2 m of subsidence in the past ~120 ka, then estimated LIG paleo-sea levels based on patch reefs and beach vugs range from ~6 to ~16.3 m above present, with most falling between ~7 and ~11.6 m (Fig. 14). With current data available, Bermuda and the Bermuda Rise appear not to have experienced any subsidence at all in the past ~40 Ma (Vogt and Jung, 2007), so no correction has been applied to the measurements shown in Fig. 15.

7.4. Comparison of LIG sea level on the Bahamas with GIA models

Although LIG paleo-sea levels, as affected by GIA processes, are modeled by Dutton and Lambeck (2012), Lambeck et al. (2012), and Dendy et al. (2017), we draw specific comparisons to those presented by Creveling et al. (2015) because the latter investigators provide four scenarios in their modeling. These include consideration of a eustatic component of +6 m of sea-level equivalent (referred to as "collapse scenario #1") as well as a eustatic component of +8 m of sea-level equivalent (referred to as "collapse scenario #2"). Further, Creveling et al. (2015) considered the response of sea level to GIA processes at both the beginning (set at ~127 ka) and end (set at ~120 ka) of the LIG period. For the Bahamas, at the beginning of the LIG, sea level is modeled to be +4.0 m (collapse scenario #1) or +6.0 m (collapse scenario #2). Under both scenarios, paleo-sea level is higher at the end of the LIG than the beginning (+9.5 m under collapse scenario #1; +11.5 m under collapse scenario #2). These modeled estimates yield an envelope of possible elevations of sea level indicators that can be compared to our field data from New Providence Island.

Unadjusted (for subsidence) field elevations show generally good agreement with GIA model estimates under either collapse scenario, with both beach ridge elevations and patch reef elevations (corrected for habitat depth) falling within the modeled envelope (Fig. 14). Agreement is not as good under collapse scenario #1 if paleo-sea levels are adjusted for subsidence of ~2 m since ~120 ka. There are two localities, however, where under any scenario, estimated paleo-sea levels for the LIG are higher than what is modeled. At NPI-78, on the western part of the island, vugs in beach sediments are as high as 14.3 m and paleo-sea level could have been as high as 16.3 m above present if subsidence is considered. At Lyford Cay, also on the western part of the island, beach vugs in both unit "ii" and unit "iii" are ~11 m above sea level (~13 m, if adjusted for subsidence), and the consistency of ages in both units as well as in the eolian facies that are derived from them gives us confidence that there is not a geochronology problem. Because both NPI-78 and Lyford Cay are on the western part of the island and elevations are generally lower in the eastern part of the island (Fig. 14), one could infer that there may have been island-wide tilt to the east, a local effect that might not be captured in the global-scale modeling presented by Creveling et al. (2015). Because of where the Bahamas are situated with respect to plate boundaries (Fig. 1),

we would not have thought it likely that tectonic activity has played a role in generating west-to-east tilt, although tectonic tilt during the Quaternary has been proposed elsewhere in the Bahamas (Kindler et al., 2011). If tectonic tilt on NPI has occurred, then the apparent ~105 ka open-system age (corresponding to the next-youngest high-sea stand of MIS 5.3) of the oolite at Clifton Pier (NPI-86) could be real and a manifestation of localized tilt to the east.

7.5. Comparison of LIG sea level on Bermuda with GIA models

For Bermuda, field estimates of LIG paleo-sea level show both agreement and disagreement with the GIA modeling. Because it is farther north and closer to that part of North America affected by the Laurentide Ice Sheet, all models indicate that Bermuda, during the LIG, should have the highest relative sea level of any island in the western Atlantic/Caribbean region (Dutton and Lambeck, 2012; Lambeck et al., 2012; Creveling et al., 2015; Dendy et al., 2017). According to the Creveling et al. (2015) model, under either collapse scenario, the start of the LIG on Bermuda should have seen a paleo-sea level ~5 m higher than present, and at the end of the LIG, paleo-sea levels of +11.3 and + 13.0 m are modeled (Fig. 15). All localities we studied on Bermuda fall well below the maximum predicted paleo-sea level at the end of the LIG (at ~120 ka) and many even fall below the lower modeled sea level of the beginning of the LIG (at ~127 ka). The highest elevations of LIG deposits we measured are ~6 m to ~7 m, and after island-wide surveys, we are not aware of any higher-elevation, confidently dated LIG deposits. Because most corals we have analyzed from Bermuda are younger than ~120 ka, in principle it could be argued that the Devonshire marine fossils are actually recording only the *fall* of sea level, into the first part of MIS 5.4. Although this is a remote possibility, it does not explain why there is no record of higher sea level, from the period of ~127 to ~120 ka. If the Hearty (2002) hypothesis of the Belmont Formation being of early LIG age is correct, that could reconcile these findings, with an interpretation that the Belmont Formation is of early LIG age and the Devonshire is of late LIG age. However, all corals collected from the Belmont Formation date to ~200 ka (Harmon et al., 1983; Muhs et al., 2002; Rowe et al., 2014). Thus, it is clear from three separate geochronology studies that the Belmont Formation is much older than the Devonshire and dates to the MIS 7 high-sea stand. Furthermore, the highest paleo-sea levels reported for the Belmont Formation are no higher than ~6 m, not substantially different from the Devonshire member (Rowe et al., 2014) and certainly much lower than the modeled +11 to +13 m levels.

There is independent evidence that sea level never reached elevations as high as +11 to +13 m from the geologic record on Bermuda. On the headland where an old British fort was situated, near Devonshire Bay (Fig. 8), an exposure ~50 m inland from the coast shows topset beds of the eolianite facies of the Belmont Formation (~200 ka), the Shore Hills paleosol developed on it, and the Rocky Bay Formation (eolianite facies, ~120 ka) at the top (Fig. 16a). The top of the headland is ~12 m above sea level and the paleosol is between ~9 and ~12 m above sea level (Land and Mackenzie, 1970, their Fig. 8), probably around 10−11 m elevation. Had the LIG sea level, during Devonshire time, reached elevations of 11−13 m above present sea level, the Shore Hills paleosol surely would have been eroded away, along with some of the topset beds of the underlying Belmont Formation. However, the paleosol still shows easily recognizable morphology (Fig. 16b) and topset beds of the Belmont Formation are still in evidence (Fig. 16a). These observations are therefore consistent with our interpretation that the LIG Devonshire marine member did not reach elevations substantially higher than ~7 m on Bermuda.

The results from Bermuda presented here are surprising, particularly in view of the fact that observations of the ~80 ka (MIS 5.1) high-sea stand on this island agree well with GIA models (Potter and Lambeck, 2003). The marine facies of the Southampton Formation (Vacher et al., 1989) is exposed at Fort St. Catherine and consists of 1−2 m of bedded, fossiliferous marine deposits overlain by a minimally developed paleosol, and the paleosol is capped by eolianite (Fig. 17a, b, c). This is essentially the same sequence of deposits found within the Rocky Bay Formation (Fig. 9a), so we do not consider the Southampton marine beds to be storm deposits, as has been suggested by other investigators (see discussion and rebuttal of this concept by Vacher and Hearty, 1989, and Muhs et al., 2002). We measured the elevation of the marine beds at Fort St. Catherine along its extent and it varies between ~1 and ~2 m above sea level. Ludwig et al. (1996) reported four U-series ages of *Oculina* corals from this unit that gave ages of ~82 to ~77 ka. Muhs et al. (2002) collected an additional 17 *Oculina* corals from the deposit and U-series ages range from ~84 to ~78 ka (Fig. 17d). We recalculated these ages using the newer estimates of half-lives of ^{230}Th and ^{234}U (Cheng et al., 2013) and the range of ages is unchanged (~84-78 ka), with all but one specimen having initial ^{234}U/^{238}U values of 1.141−1.1539. A further set of calculations using the Thompson et al. (2003) method of open-system age calculation yields an age range of 85.3 to 77.9 ka. Thus, there is little question that Fort St. Catherine records a high-sea stand above present at ~80 ka (MIS 5.1) on Bermuda. This conclusion is supported by a recent study of speleothems on Bermuda, where a growth hiatus just prior to ~80 ka is interpreted to be due to sea level rise above present (Wainer et al., 2017).

Potter and Lambeck (2003) pointed out that there is a systematic, southward decrease in elevations of ~80 ka marine deposits from Virginia and the Carolinas (Wehmiller et al., 2004) to Bermuda (Muhs et al., 2002) to the Florida Keys (Ludwig et al., 1996) to Haiti (corrected for uplift by Dodge et al., 1983), and finally to Barbados (corrected for uplift by Broecker et al., 1968). This trend of southward-decreasing paleo-sea level estimates for the high stand at ~80 ka (MIS 5.1) fits GIA modeling because of the southward-decreasing influence of the Laurentide Ice Sheet (Potter and Lambeck, 2003). More recent modeling by Creveling et al. (2017) is consistent with the earlier results of Potter and Lambeck (2003), with a prediction of a higher-than-present sea level on Bermuda at ~80 ka. Thus, it is not clear why there is such good agreement with GIA models for Bermuda for the ~80 ka high-sea stand and not the ~120 ka high-sea stand.

7.6. Comparison of LIG sea level in Florida with GIA models

Because of their proximity to the Bahamas, it is also worthwhile testing GIA models of LIG sea level on the Florida Keys and Florida mainland (Fig. 1). For this, we use the elevation and age data reported by Muhs et al. (2011). Oolites are present in the Miami area of the Florida mainland, coral reefs are present in the Upper Florida Keys, and oolites are present in the Lower Florida Keys. Although oolite ages are tentative, they appear to have the same linear trend on an isotopic evolution diagram as LIG ooids on New Providence Island (Fig. 12b). As mentioned above, we recalculated open-system ages for corals from the Upper Florida Keys and with two somewhat older exceptions, the other 38 corals fall into an age range of ~132 to ~111 ka. Thus, all these samples can be considered to represent the LIG period.

Using Florida corals and oolites as paleo-sea level indicators is somewhat more challenging. Although Muhs et al. (2011) reported one *Acropora palmata* specimen from Windley Key, Florida, it was not in growth position. All growth-position corals we have observed on the Florida Keys are species of *Orbicella*, *Montastraea*,
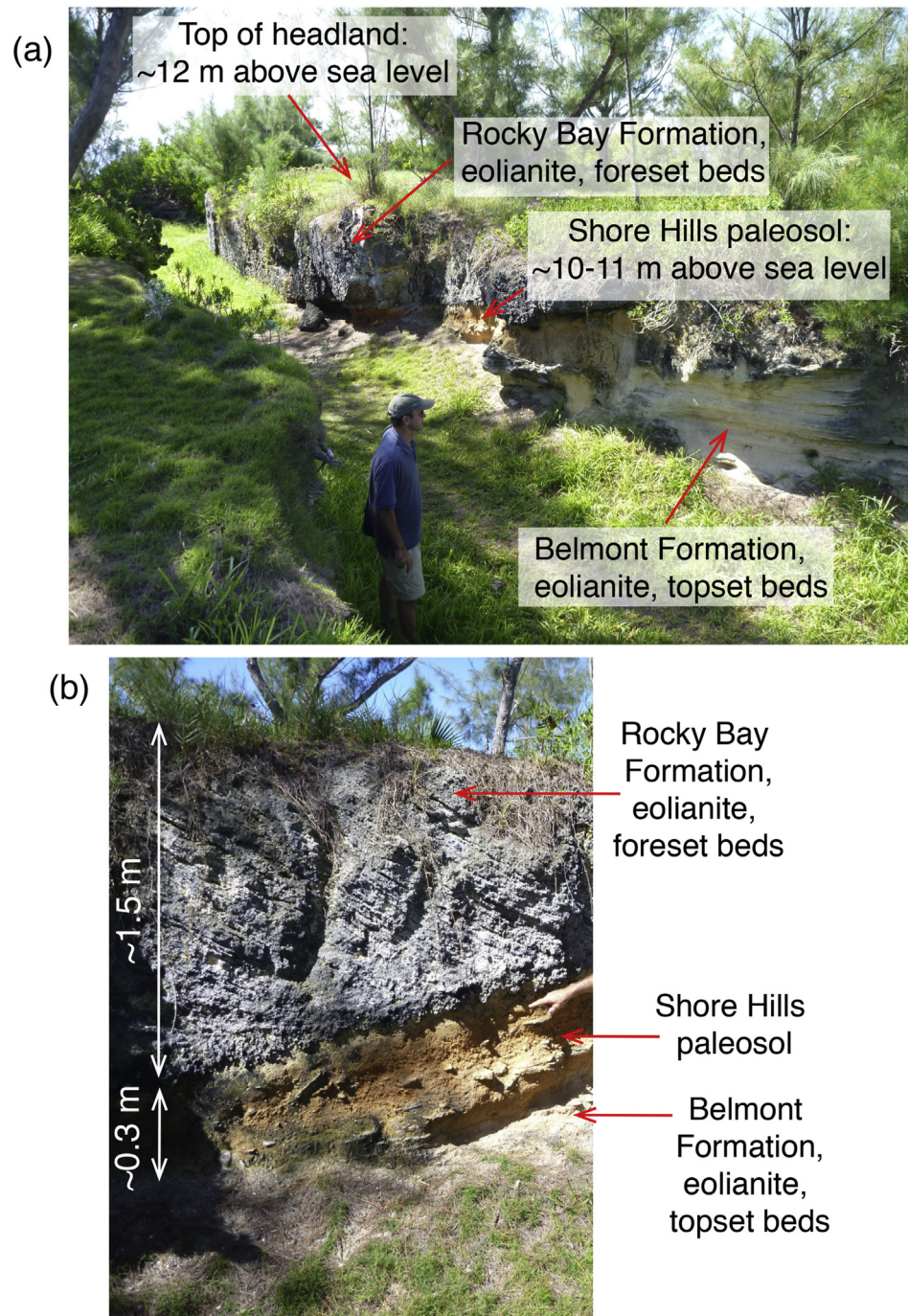
Fig. 16. Photographs of the Devonshire Bay area of Bermuda (see Fig. 8 for location), near the old British fort, showing (a) exposure of the Rocky Bay Formation (eolianite), the "Shore Hills" paleosol, and the Belmont Formation (eolianite) and (b) detail of cross-bedded eolianite of the Rocky Bay Formation and the Shore Hills paleosol. Note that the elevation at the top of the headland where these exposures are found is ~12 m above sea level, with the paleosol found at ~10 m to ~11 m above sea level. Photographs by D.R. Muhs.

Colpophyllia, and *Diploria* which, as noted above, all have considerable depth-habitat ranges. Thus, as with the patch reef corals in growth position on New Providence Island, we have added a *minimum* depth of ~3 m for where these corals lived during the LIG (Fig. 18).

A challenge also exists for estimating paleo-sea level from oolites in Florida. Unlike New Providence Island, Florida oolites do not have a geomorphic or sedimentologic expression that indicates the sediments were deposited as beach ridges, close to sea level. It is more likely that they were deposited as ooid shoals, likely as bank or bar systems (Halley et al., 1997). Based on studies of modern ooids in the Bahamas, these sediments could have formed in water near sea level or as deep as ~3.3 m (Newell et al., 1960). The problem is compounded by the fact that ooids could have been transported some considerable distance laterally or to deeper or shallower waters than those in which they precipitated. Hence, we have assigned a *possible* depth adjustment of ~3 m (the deepest water in which ooids form at present in the Bahamas) to the measured elevations of Muhs et al. (2011) for Florida oolites.

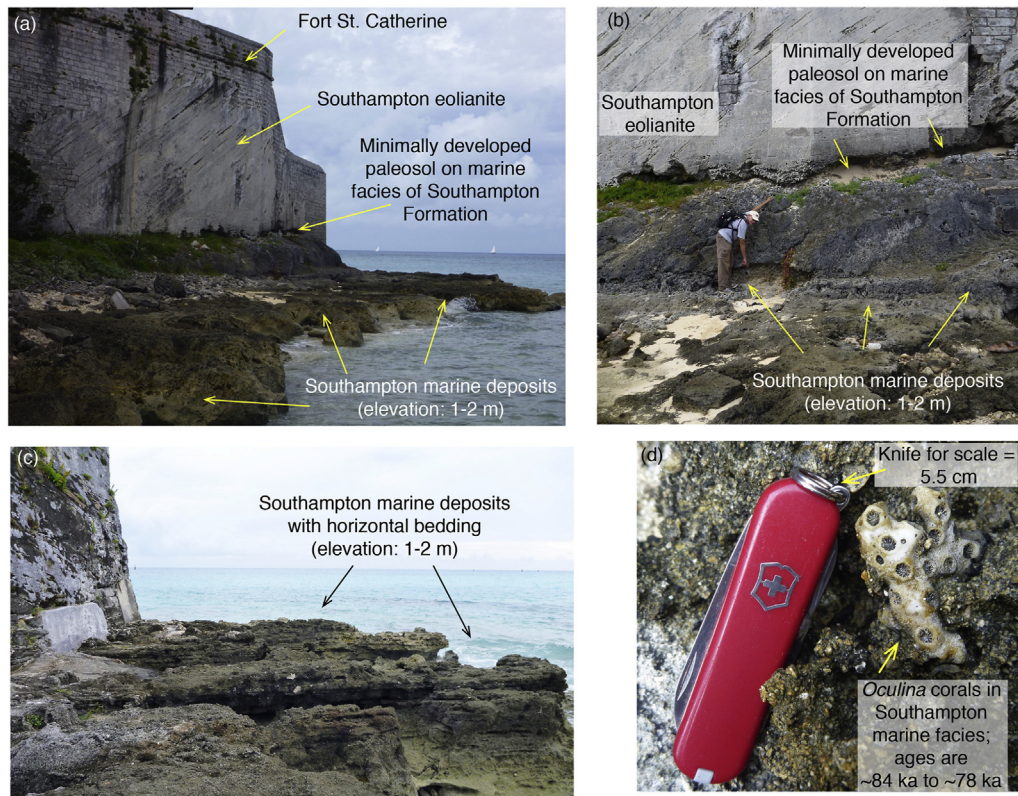Finally, as is the case with the Bahamas, it is likely that Florida

Fig. 17. Photographs of the Fort St. Catherine area of Bermuda (see Fig. 8 for location), showing (a) overall stratigraphy of the Southampton Formation exposed under the fort; (b) details of the contacts between the marine deposits, overlying paleosol, and overlying eolianite; (c) bedding within the marine deposits of the Southampton Formation; and (d) typical *Oculina* coral colony found within the Southampton Formation marine deposits, similar to those dated to ~84 to ~78 ka by Muhs et al. (2002). Photographs by D.R. Muhs.

has experienced long-term subsidence. Using the Lynts (1970) subsidence graph for the Florida Keys, we estimate ~345 m of subsidence in ~37.5 Ma (since the late Eocene). This yields a subsidence rate of ~0.0092 m/ka, or ~1.1 m of subsidence in the past ~120 ka. Thus, in Fig. 18, we plot both (1) measured elevations, with corrections for habitat depth (corals) or depth of formation (ooids), and (2) measured elevations with the same depth corrections *and* a 1-m correction for long-term subsidence.

Comparison of the field results for Florida with modeled GIA paleo-sea levels by Creveling et al. (2015) indicates partial agreement. Under collapse scenario #1 (+6 m eustatic level), most Florida localities have measured elevations (or *permitted* elevations, with adjustments) that fall within or close to the envelope for modeled LIG sea level (Fig. 18a). Under collapse scenario #2 (+8 m eustatic level), a number of localities, except those in the Miami area, fall well below the envelope of modeled paleo-sea levels for the LIG (Fig. 18b). Thus, as with the Bahamas, there is some agreement with modeled paleo-sea levels for the Florida Keys (scenario #1), but as with Bermuda, there are underestimates as well (scenario #2).

8. Conclusions

It is now well established that where coastlines would have been affected by GIA processes due to the presence of the Laurentide Ice Sheet during the past two glacial periods, there may be geologic records of high sea levels that differ from those expected from purely eustatic considerations. Thus, the tectonically stable islands of the Bahamas are modeled to have had a maximum last interglacial (LIG) sea level of ~9.5–11.5 m above the present, and Bermuda is modeled to have had a maximum LIG sea level stand of

~11–13 m above the present. GIA models such as these, however, require testing with geologic records. The present study was undertaken to provide such tests, from the tectonically stable islands of the Bahamas and Bermuda.

Corals from patch reefs on New Providence Island, Bahamas, have U-series ages with minimal bias ranging from ~128 to ~118 ka, and ooids/peloids from beach ridges have ages with minimal bias ranging from of ~128 to ~116 ka, all well within the LIG. Open-system age calculations for other corals and ooids are in agreement with these age ranges. The elevations of the patch reefs indicate a LIG paleo-sea level of at least 7.4–8.8 m above present sea level when adjusted conservatively for habitat depth and long-term subsidence. Beach ridge sediments, marked by the presence of vugs, form close to sea level. Elevations of these features on New Providence Island indicate paleo-sea levels of ~5 m to ~14 m above present during the LIG, or ~7 m to ~16 m when adjusted for long-term subsidence. Some, though not all of these measurements are in good agreement with GIA models of paleo-sea level that have been simulated for the Bahamas. Examination of published elevations of emergent coral reefs and oolitic marine deposits of LIG age from Florida show similar results to those from New Providence Island.

We find less agreement with GIA models from geologic records of the LIG on Bermuda. Corals from emergent marine deposits have minimally biased ages ranging from ~126 to ~114 ka, in good agreement with ages of corals and ooids from New Providence Island. Although emergent marine deposits on Bermuda lack the precise indication of paleo-sea level provided by patch reefs and oolitic beach ridges with vugs, these sediments nevertheless provide at least a minimum-limiting estimate of paleo-sea level. Elevation measurements indicate, however, that paleo-sea level
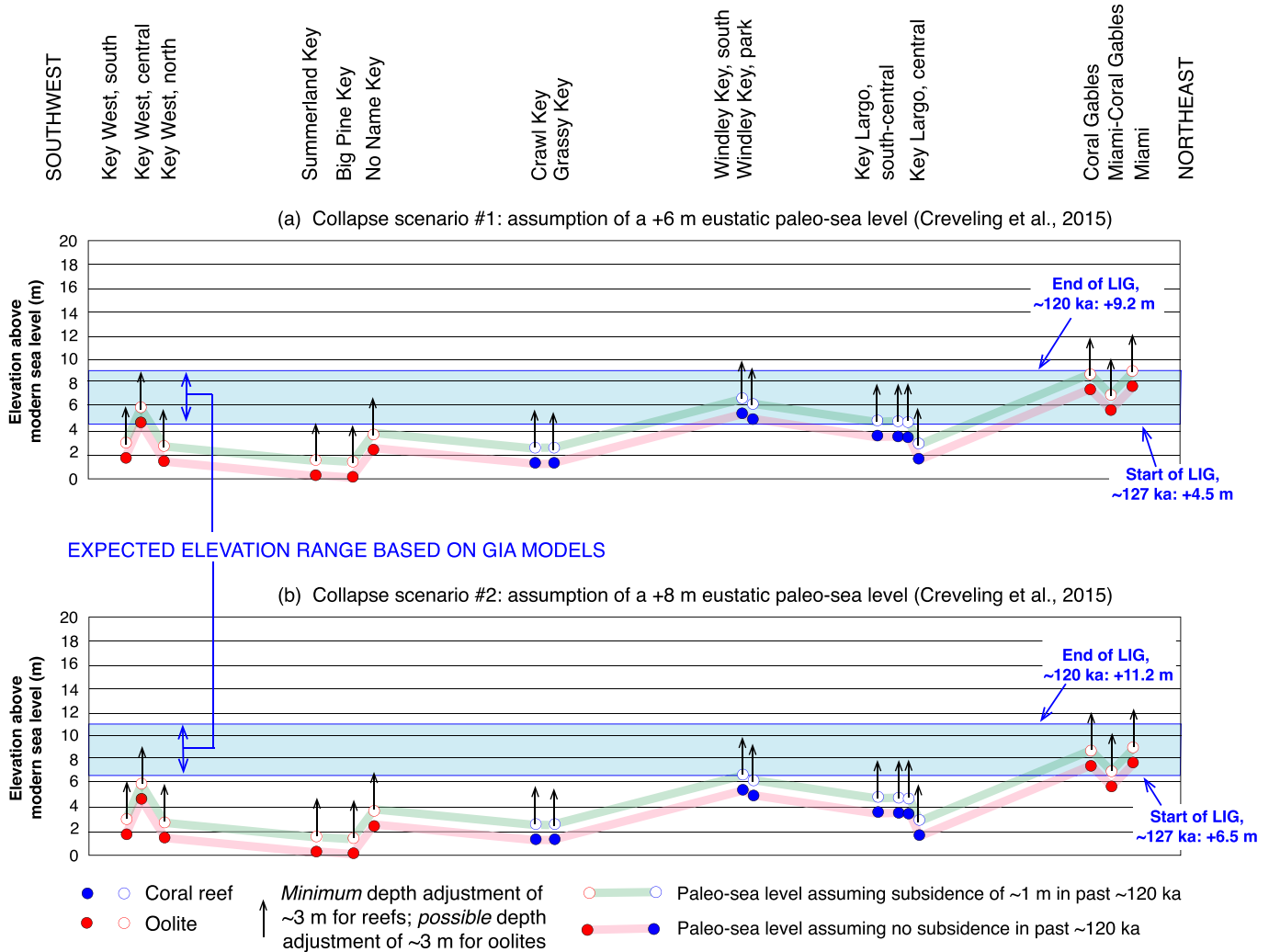
Fig. 18. Shore-parallel profiles, showing GPS-derived elevations of oolitic marine sediments (filled red circles) and coral-bearing marine sediments (filled blue circles) on the Florida Keys and in the Miami, Florida area. Locality names and elevations are from Fig. 11 of Muhs et al. (2011); all sediments are considered to have been deposited during the last interglacial period, based on U-series data in Muhs et al. (2011), their Tables 1 and 2. Arrows on coral reef symbols indicate *minimum* corrections, assuming that reefs grew in at least 3 m of water, based on the present *optimal* habitat depths of coral taxa identified (Shinn et al., 1989; see also Hibbert et al., 2016). Arrows on oolite sediment elevations show *possible* corrections, based on modern observations of ooid formation in water depths of up to 3.3 m in the Bahamas (Newell et al., 1960). Blue shade in (a) represents GIA-modeled range of sea level at the beginning (~127 ka) and end (~120 ka) of the last-interglacial (LIG) high-sea stand, assuming a +6 m eustatic paleo-sea level ("collapse scenario #1" of Creveling et al., 2015). Panel (b) is the same as in (a) except the range of the last-interglacial (LIG) high-sea stand assumes a +8 m eustatic paleo-sea level ("collapse scenario #2" of Creveling et al., 2015). Also shown in both (a) and (b), with open circles, are paleo-sea level estimates based on measured elevations as described above, but also with adjustment of long-term subsidence of ~1 m in the past ~120 ka (see text for discussion). (For interpretation of the references to color in this figure legend, the reader is referred to the Web version of this article.)

records on Bermuda are consistently lower than what GIA models simulate for the LIG in this region of the western Atlantic. The results are surprising, particularly in view of the fact that the geologic record of marine deposits from Bermuda is in good agreement with GIA modeling for the later, ~80 ka high-sea stand. The reason for the reasonable agreement with LIG models for the Bahamas and Florida and poor agreement for Bermuda is not understood and needs more study. A potentially fruitful effort to provide additional tests of GIA models could come from studies of other coastlines in tectonically stable regions. The Atlantic Coastal Plain of the eastern USA is an obvious target, as are other islands of the Bahamas, and the eastern coast of South America.

References

Barlow, N.L.M., McClymont, E.L., Whitehouse, P.L., Stokes, C.R., Jamieson, S.S.R., Woodroffe, S.A., Bentley, M.J., Callard, S.L., Ó Cofaigh, C., Evans, D.J.A., Horrocks, J.R., Lloyd, J.M., Long, A.J., Margold, M., Roberts, D.H., Sanchez-Montes, M.L., 2018. Lack of evidence for a substantial sea-level fluctuation within the Last Interglacial. Nat. Geosci. 11, 627–634.

Bloom, A.L., Broecker, W.S., Chappell, J.M.A., Matthews, R.K., Mesolella, K.J., 1974. Quaternary sea level fluctuations on a tectonic coast: new ^{230}Th/^{234}U dates from the Huon Peninsula, New Guinea. Quat. Res. 4, 185–205.

Broecker, W.S., Thurber, D.L., 1965. Uranium-series dating of corals and oolites from Bahaman and Florida Key limestones. Science 149, 58–60.

Broecker, W.S., Thurber, D.L., Goddard, J., Ku, T.-L., Matthews, R.K., Mesolella, K.J., 1968. Milankovitch hypothesis supported by precise dating of coral reefs and deep-sea sediments. Science 159, 297–300.

Carew, J.L., Mylroie, J.E., 1997. Geology of the Bahamas. In: Vacher, H.L., Quinn, T.M. (Eds.), Geology and Hydrology of Carbonate Islands. Developments in Sedimentology 54. Elsevier, Amsterdam, pp. 91–139.

Chappell, J., 1974. Geology of coral terraces, Huon Peninsula, New Guinea: a study of Quaternary tectonic movements and sea-level changes. Geol. Soc. Am. Bull. 85, 553–570.

Chappell, J., Veeh, H.H., 1978. Late Quaternary tectonic movements and sea-level changes at timor and Atauro island. Geol. Soc. Am. Bull. 89, 356–368.

Chen, J.H., Edwards, R.L., Wasserburg, G.J., 1986. ^{238}U, ^{234}U, and ^{232}Th in seawater. Earth Planet Sci. Lett. 80, 241–251.

Chen, J.H., Curran, H.A., White, B., Wasserburg, G.J., 1991. Precise chronology of the last interglacial period: ^{234}U-^{230}Th data from fossil coral reefs in the Bahamas. Geol. Soc. Am. Bull. 103, 82–97.

Cheng, H., Edwards, R.L., Shen, C.-C., Polyak, V.J., Asmerom, Y., Woodhead, J., Hellstrom, J., Wang, Y., Kong, X., Spötl, C., Wang, X., Alexander Jr., E.C., 2013. Improvements in ^{230}Th dating, ^{230}Th and ^{234}U half-life values, and U-Th isotopic measurements by multi-collector inductively coupled plasma mass spectrometry. Earth Planet Sci. Lett. 371–372, 82–91.

Chung, G.S., Swart, P.K., 1990. The concentration of uranium in freshwater vadose and phreatic cements in a Holocene ooid cay: a method of identifying ancient water tables. J. Sediment. Petrol. 60, 735–746.

Church, J.A., Clark, P.U., Cazenave, A., Gregory, J.M., Jevrejeva, S., Levermann, A., Merrifield, M.A., Milne, G.A., Nerem, R.S., Nunn, P.D., Payne, A.J., Pfeffer, W.T., Stammer, D., Unnikrishnan, A.S., 2013. Sea level change. In: Stocker, T.F., Qin, D., Plattner, G.-K., Tignor, M., Allen, S.K., Boschung, J., Nauels, A., Xia, Y., Bex, V., Midgley, P.M. (Eds.), Climate Change 2013: the Physical Science Basis. Contribution of Working Group I to the Fifth Assessment Report of the Intergovernmental Panel on Climate Change. Cambridge University Press, Cambridge, United Kingdom and New York, NY, USA, pp. 1137–1216.

Cohen, A.L., Branch, G.M., 1992. Environmentally controlled variation in the structure and mineralogy of Patella granularis shells from the coast of southern Africa: implications for palaeotemperature assessments. Palaeogeogr. Palaeoclimatol. Palaeoecol. 91, 49–57.

Creveling, J.R., Mitrovica, J.X., Hay, C.C., Austermann, J., Kopp, R.E., 2015. Revisiting tectonic corrections applied to Pleistocene sea-level highstands. Quat. Sci. Rev. 111, 72–80.

Creveling, J.R., Mitrovica, J.X., Clark, P.U., Waelbroeck, C., Pico, T., 2017. Predicted bounds on peak global mean sea level during marine isotope stages 5a and 5c. Quat. Sci. Rev. 163, 193–208.

Cross, T.S., Cross, B.W., 1983. U, Sr, and Mg in Holocene and Pleistocene corals A. palmata and M. annularis. J. Sediment. Petrol. 53, 587–594.

Cutler, K.B., Edwards, R.L., Taylor, F.W., Cheng, H., Adkins, A., Gallup, C.D., Cutler, P.M., Burr, G.S., Bloom, A.L., 2003. Rapid sea-level fall and deep-ocean temperature change since the last interglacial period. Earth Planet Sci. Lett. 206, 253–271.

Dean, W.E., 2009. Endogenic carbonate sedimentation in Bear Lake, Utah and Idaho, over the last two glacial-interglacial cycles. Geol. Soc. Am. Spec. Pap. 450, 169–196.

Dean, W.E., Forester, R.M., Bright, J., Anderson, R.Y., 2007. Influence of the diversion of Bear River into Bear Lake (Utah and Idaho) on the environment of deposition of carbonate minerals. Limnol. Oceanogr. 52, 1094–1111.

Delanghe, D., Bard, E., Hamelin, B., 2002. New TIMS constraints on the uranium-238 and uranium-234 in seawaters from the main ocean basins and the Mediterranean Sea. Mar. Chem. 80, 79–93.

Dendy, S., Austermann, J., Creveling, J.R., Mitrovica, J.X., 2017. Sensitivity of Last Interglacial sea-level high stands to ice sheet configuration during Marine Isotope Stage 6. Quat. Sci. Rev. 171, 234–244.

Dodge, R.E., Fairbanks, R.G., Benninger, L.K., Maurrasse, F., 1983. Pleistocene sea levels from raised coral reefs of Haiti. Science 219, 1423–1425.

Dutton, A., Carlson, A.E., Long, A.J., Milne, G.A., Clark, P.U., DeConto, R., Horton, B.P., Rahmstorf, S., Raymo, M.E., 2015a. Sea-level rise due to polar ice-sheet mass loss during past warm periods. Science 349. https://doi.org/10.1126/science.aaa4019.

Dutton, A., Lambeck, K., 2012. Ice volume and sea level during the last interglacial. Science 337, 216–219.

Dutton, A., Webster, J.M., Zwartz, D., Lambeck, K., Wohlfarth, B., 2015b. Tropical tales of polar ice: evidence of Last Interglacial polar ice sheet retreat recorded by fossil reefs of the granitic Seychelles islands. Quat. Sci. Rev. 107, 182–196.

Edwards, R.L., Cheng, H., Murrell, M.T., Goldstein, S.J., 1997. Protactinium-231 dating

of carbonates by thermal ionization mass spectrometry: implications for Quaternary climate change. Science 276, 782–786.

Gallup, C.D., Edwards, R.L., Johnson, R.G., 1994. The timing of high sea levels over the past 200,000 years. Science 263, 796–800.

Gallup, C.D., Cheng, H., Taylor, F.W., Edwards, R.L., 2002. Direct determination of the timing of sea level change during Termination II. Science 295, 310–313.

Garrett, P., Gould, S.J., 1984. Geology of new providence island, Bahamas. Geol. Soc. Am. Bull. 95, 209–220.

Goreau, T.F., 1959. The ecology of Jamaican coral reefs. I. Species composition and zonation. Ecology 40, 67–90.

Goreau, T.F., Goreau, N.I., 1973. The ecology of Jamaican coral reefs. II. Geomorphology, zonation, and sedimentary phases. Bull. Mar. Sci. 23, 399–464.

Government of the Commonwealth of the Bahamas, 1988. Hydrographic Chart of the Commonwealth of the Bahamas, 2nd Edition. Scale, 1:250,000., 1 Government of the Commonwealth of the Bahamas.

Gupta, S.K., 1972. Chronology of the raised beaches and inland coral reefs of the Saurashtra coast. J. Geol. 80, 357–361.

Halley, R.B., Harris, P.M., 1979. Fresh-water cementation of a 1,000-year-old oolite. J. Sediment. Petrol. 49, 969–988.

Halley, R.B., Harris, P.M., Hine, A.C., 1983. Bank margin environment. In: Scholle, P.A., Bebout, D.G., Moore, C.H. (Eds.), Carbonate Depositional Environments. Memoirs of the American Association of Petroleum Geologists 33, pp. 463–506.

Halley, R.B., Vacher, H.L., Shinn, E.A., 1997. Geology and hydrogeology of the Florida Keys. In: Vacher, H.L., Quinn, T.M. (Eds.), Geology and Hydrology of Carbonate Islands. Developments in Sedimentology, vol. 54. Elsevier, Amsterdam, pp. 217–248.

Harmon, R.S., Mitterer, R.M., Kriausakul, N., Land, L.S., Schwarcz, H.P., Garrett, P., Larson, G.J., Vacher, H.L., Rowe, M., 1983. U-series and amino-acid racemization geochronology of Bermuda: implications for eustatic sea-level fluctuation over the past 250,000 years. Palaeogeogr. Palaeoclimatol. Palaeoecol. 44, 41–70.

Hay, C., Mitrovica, J.X., Gomez, N., Creveling, J.R., Austermann, J., Kopp, R.E., 2014. The sea-level fingerprints of ice-sheet collapse during interglacial periods. Quat. Sci. Rev. 87, 60–69.

Hearty, P.J., 2002. Revision of the late Pleistocene stratigraphy of Bermuda. Sedimentology 153, 1–21.

Hearty, P.J., Kindler, P., 1997. The stratigraphy and surficial geology of New Providence and surrounding islands, Bahamas. J. Coast Res. 13, 798–812.

Hibbert, F.D., Rohling, E.J., Dutton, A., Williams, F.H., Chutcharavan, P.M., Zhao, C., Tamisiea, M.E., 2016. Coral indicators of past sea-level change: a global repository of U-series dated benchmarks. Quat. Sci. Rev. 145, 1–56.

Inden, R.F., Moore, C.H., 1983. Beach environment. In: Scholle, P.A., Bebout, D.G., Moore, C.H. (Eds.), Carbonate Depositional Environments. Memoirs of the American Association of Petroleum Geologists 33, pp. 211–265.

Kaufman, A., Broecker, W.S., Ku, T.-L., Thurber, D.L., 1971. The status of U-series methods of mollusk dating. Geochem. Cosmochim. Acta 35, 1155–1183.

Kindler, P., Godefroid, F., Chiaradia, M., Ehlert, C., Eisenhauer, A., Frank, M., Hasler, C.-A., Samankassou, E., 2011. Discovery of Miocene to early Pleistocene deposits on Mayguana, Bahamas: evidence for recent active tectonism on the North American margin. Geology 39, 523–526.

Kopp, R.E., Simons, F.J., Mitrovica, J.X., Maloof, A.C., Oppenheimer, M., 2009. Probabilistic assessment of sea level during the last interglacial stage. Nature 462, 863–868.

Kopp, R.E., Simons, F.J., Mitrovica, J.X., Maloof, A.C., Oppenheimer, M., 2013. A probabilistic assessment of sea level variations within the last interglacial stage. Geophys. J. Int. 193, 711–716.

Ku, T.-L., Kimmel, M.A., Easton, W.H., O'Neil, T.J., 1974. Eustatic sea level 120,000 years ago on Oahu, Hawaii. Science 183, 959–962.

Lambeck, K., Purcell, A., Dutton, A., 2012. The anatomy of interglacial sea levels: the relationship between sea levels and ice volumes during the Last Interglacial. Earth Planet Sci. Lett. 315–316, 4–11.

Land, L.S., Mackenzie, F.T., 1970. Field Guide to Bermuda Geology. Bermuda Biological Station for Research Special Publication 4.

Land, L.S., Mackenzie, F.T., Gould, S.J., 1967. Pleistocene history of Bermuda. Geol. Soc. Am. Bull. 78, 993–1006.

Lowenstam, H.A., 1954. Factors affecting the aragonite:calcite ratios in carbonate-secreting marine organisms. J. Geol. 62, 284–322.

Ludwig, K.R., 2001. In: Users Manual for Isoplot/Ex, Rev. 2.49. Berkeley Geochronology Center, Berkeley, California, Special Publication.

Ludwig, K.R., Paces, J.B., 2002. Uranium-series dating of pedogenic silica and carbonate, Crater Flat, Nevada. Geochem. Cosmochim. Acta 66, 487–506.

Ludwig, K.R., Wallace, A.R., Simmons, K.R., 1985. The Schwartzwalder uranium deposit, II: age of uranium mineralization and Pb-isotope constraints on genesis. Econ. Geol. 80, 1858–1871.

Ludwig, K.R., Simmons, K.R., Szabo, B.J., Winograd, I.J., Landwehr, J.M., Riggs, A.C., Hoffman, R.J., 1992. Mass-spectrometric ^{230}Th-^{234}U-^{238}U dating of the Devils Hole calcite vein. Science 258, 284–287.

Ludwig, K.R., Muhs, D.R., Simmons, K.R., Halley, R.B., Shinn, E.A., 1996. Sea level records at ~80 ka from tectonically stable platforms: Florida and Bermuda. Geology 24, 211–214.

Lynts, G.W., 1970. Conceptual model of the Bahamian Platform for the last 135 million years. Nature 225, 1226–1228.

Mackenzie, F.T., 1964a. Bermuda Pleistocene eolianites and paleowinds. Sedimentology 3, 52–64.

Mackenzie, F.T., 1964b. Geometry of Bermuda calcareous dune cross-bedding. Science 144, 1449–1450.

Magaritz, M., Gavish, E., Bakler, N., Kafri, U., 1979. Carbon and oxygen isotope composition—Indicators of cementation environment in Recent, Holocene, and Pleistocene sediments along the coast of Israel. J. Sediment. Petrol. 49, 401—412.

Mann, P., 2007. Global catalogue, classification and tectonic origins of restraining- and releasing bends on active and ancient strike-slip fault systems. Geol. Soc. Lond. Special Publ. 290, 13—142.

Martin, L., Suguio, K., Flexor, J.-M., 1988. Hauts niveaux marins Pleistocenes du littoral Bresilien. Palaeogeogr. Palaeoclimatol. Palaeoecol. 68, 231—239.

Martinson, D.G., Pisias, N.G., Hays, J.D., Imbrie, J., Moore Jr., T.C., Shackleton, N.J., 1987. Age dating and the orbital theory of the ice ages: development of a high-resolution 0 to 300,000-year chronostratigraphy. Quat. Res. 27, 1—29.

McNeill, D.F., Ginsburg, R.N., Chang, S.-B.R., Kirschvink, J.L., 1988. Magnetostratigraphic dating of shallow-water carbonates from San Salvador. Bahamas. Geol. 16, 8—12.

Meischner, D., Vollbrecht, R., Wehmeyer, D., 1995. Pleistocene sea-level yo-yo recorded in stacked beaches, Bermuda south shore. Geol. Soc. Am. Spec. Pap. 300, 295—310.

Melim, L.A., Masaferro, J.L., 1997. Geology of the Bahamas: subsurface geology of the Bahamas banks. In: Vacher, H.L., Quinn, T.M. (Eds.), Geology and Hydrology of Carbonate Islands. Developments in Sedimentology 54. Elsevier, Amsterdam, pp. 161—182.

Muhs, D.R., 2002. Evidence for the timing and duration of the last interglacial period from high-precision uranium-series ages of corals on tectonically stable coastlines. Quat. Res. 58, 36—40.

Muhs, D.R., Simmons, K.R., 2017. Taphonomic problems in reconstructing sea-level history from the late Quaternary marine terraces of Barbados. Quat. Res. 88, 409—429.

Muhs, D.R., Simmons, K.R., Steinke, B., 2002. Timing and warmth of the last interglacial period: new U-series evidence from Hawaii and Bermuda and a new fossil compilation for North America. Quat. Sci. Rev. 21, 1355—1383.

Muhs, D.R., Budahn, J.R., Prospero, J.M., Skipp, G., Herwitz, S., 2012a. Soil genesis on the island of Bermuda in the Quaternary: the importance of African dust transport and deposition. J. Geophys. Res. 117, F03025 https://doi.org/10.1029/2012JF002366.

Muhs, D.R., Bush, C.A., Stewart, K.C., Rowland, T.R., 1990. Geochemical evidence of Saharan dust parent material for soils developed on Quaternary limestones of Caribbean and western Atlantic islands. Quat. Res. 33, 157—177.

Muhs, D.R., Budahn, J., Prospero, J.M., Carey, S.N., 2007. Geochemical evidence for African dust inputs to soils of western Atlantic islands: Barbados, the Bahamas and Florida. J. Geophys. Res. 112, F02009 https://doi.org/10.1029/2005JF000445.

Muhs, D.R., Simmons, K.R., Schumann, R.R., Groves, L.T., Mitrovica, J.X., Laurel, D., 2012b. Sea-level history during the last interglacial complex on San Nicolas Island, California: implications for glacial isostatic adjustment processes, paleozoogeography and tectonics. Quat. Sci. Rev. 37, 1—25.

Muhs, D.R., Simmons, K.R., Schumann, R.R., Halley, R.B., 2011. Sea-level history of the past two interglacial periods: new evidence from U-series dating of reef corals from south Florida. Quat. Sci. Rev. 30, 570—590.

Muhs, D.R., Meco, J., Simmons, K.R., 2014. Uranium-series ages of corals, sea level history, and palaeozoogeography, Canary Islands, Spain: an exploratory study for two Quaternary interglacial periods. Palaeogeogr. Palaeoclimatol. Palaeoecol. 394, 99—118.

Muhs, D.R., Pandolfi, J.M., Simmons, K.R., Schumann, R.R., 2012c. Sea-level history of past interglacial periods from uranium-series dating of corals, Curaçao, Leeward Antilles islands. Quat. Res. 78, 157—169.

Muhs, D.R., Schweig, E.S., Simmons, K.R., Halley, R.B., 2017. Late Quaternary uplift along the North America-Caribbean plate boundary: evidence from the sea level record of Guantanamo Bay, Cuba. Quat. Sci. Rev. 178, 54—76.

Murray-Wallace, C.V., Woodroffe, C.D., 2014. Quaternary Sea Level Changes: A Global Perspective. Cambridge University Press, Cambridge, p. 484.

Murray-Wallace, C.V., Belperio, A.P., Dosseto, A., Nicholas, W.A., Mitchell, C., Bourman, R.P., Eggins, S.M., Grün, R., 2016. Last interglacial (MIS 5e) sea-level determined from a tectonically stable, far-field location, Eyre Peninsula, southern Australia. Aust. J. Earth Sci. 63, 611—630.

Newell, N.D., Purdy, E.G., Imbrie, J., 1960. Bahamian oölitic sand. J. Geol. 68, 481—497.

O'Leary, M.J., Hearty, P.J., Thompson, W.G., Raymo, M.E., Mitrovica, J.X., Webster, J.M., 2013. Ice sheet collapse following a prolonged period of stable sea level during the last interglacial. Nat. Geosci. 6, 796—800.

Oliver, T.S.N., Murray-Wallace, C.V., Woodroffe, C.D., 2020. Holocene shoreline progradation and coastal evolution at Guichen and Rivoli Bays, southern Australia. The Holocene 30, 106—124.

Osmond, J.K., Carpenter, J.R., Windom, H.L., 1965. ^{230}Th/^{234}U age of the Pleistocene corals and oolites of Florida. J. Geophys. Res. 70, 1843—1847.

Ota, Y., Chappell, J., Kelley, R., Yonekura, N., Matsumoto, E., Nishimura, T., Head, J., 1993. Holocene coral reef terraces and coseismic uplift of Huon Peninsula, Papua New Guinea. Quat. Res. 40, 177—188.

Otto-Bliesner, B.L., Marshall, S.J., Overpeck, J.T., Miller, G.H., Hu, A., CAPE Last Interglacial Project members, 2006. Simulating Arctic climate warmth and icefield retreat in the last interglaciation. Science 311, 1751—1753.

Overpeck, J.T., Otto-Bliesner, B.L., Miller, G.H., Muhs, D.R., Alley, R.B., Kiehl, J.T., 2006. Paleoclimatic evidence for future ice-sheet instability and rapid sea-level rise. Science 311, 1747—1750.

Pindell, J.L., Kennan, L., 2009. Tectonic evolution of the Gulf of Mexico, Caribbean

and northern South America in the mantle reference frame: an update. Geol. Soc. Lond. Special Publ. 328, 1—55.

Potter, E.-K., Lambeck, K., 2003. Reconciliation of sea-level observations in the western North Atlantic during the last glacial cycle. Earth Planet Sci. Lett. 217, 171—181.

Rohling, E.J., Grant, K., Hemleben, Ch, Siddall, M., Hoogakker, B.A.A., Bolshaw, M., Kucera, M., 2008. High rates of sea-level rise during the last interglacial period. Nat. Geosci. 1, 38—42.

Rowe, M.P., 1990. An Explanation of the Geology of Bermuda. Bermuda Government, Ministry of Works & Engineering, p. 28.

Rowe, M.P., Bristow, C.S., 2015. Sea-level controls on carbonate beaches and coastal dunes (eolianite): lessons from Pleistocene Bermuda. Geol. Soc. Am. Bull. 127, 1645—1665.

Rowe, M.P., Wainer, K.A., Bristow, C.S., Thomas, A.L., 2014. Anomalous MIS 7 sea-level recorded on Bermuda. Quat. Sci. Rev. 90, 47—59.

Sayles, R.W., 1931. Bermuda during the Ice Age. Proc. Am. Acad. Arts Sci. 66, 381—468.

Schellmann, G., Radtke, U., 2004. A revised morpho- and chronostratigraphy of the Late and Middle Pleistocene coral reef terraces on southern Barbados (West Indies). Earth Sci. Rev. 64, 157—187.

Shinn, E.A., Lidz, B.H., Kindinger, J.L., Hudson, J.H., Halley, R.B., 1989. Reefs of Florida and the Dry Tortugas: A Guide to the Modern Carbonate Environments of the Florida Keys and the Dry Tortugas. U.S. Geological Survey, St. Petersburg, Florida, p. 53.

Skrivanek, A., Li, J., Dutton, A., 2018. Relative sea-level change during the Last Interglacial as recorded in Bahamian fossil reefs. Quat. Sci. Rev. 200, 160—177.

Smith, D.A., Small, H.J., 1999. The CARIB97 high-resolution geoid height model for the Caribbean Sea. J. Geodes. 73, 1—9.

Somayajulu, B.L.K., Broecker, W.S., Goddard, J., 1985. Dating Indian corals by U-decay-series methods. Quat. Res. 24, 235—239.

Speed, R.C., Cheng, H., 2004. Evolution of marine terraces and sea level in the last interglacial, Cave Hill, Barbados. Geol. Soc. Am. Bull. 116, 219—232.

Stanley, S.M., 1966. Paleoecology and diagenesis of Key largo limestone, Florida. Bull. Am. Assoc. Pet. Geol. 50, 1927—1947.

Stein, M., Wasserburg, G.J., Aharon, P., Chen, J.H., Zhu, Z.R., Bloom, A., Chappell, J., 1993. TIMS U-series dating and stable isotopes of the last interglacial event in Papua New Guinea. Geochem. Cosmochim. Acta 57, 2541—2554.

Stirling, C.H., Andersen, M.B., 2009. Uranium-series dating of fossil coral reefs: extending the sea-level record beyond the last glacial cycle. Earth Planet Sci. Lett. 284, 269—283.

Strasser, A., Davaud, E., 1986. Formation of Holocene limestone sequences by progradation, cementation, and erosion: two examples from the Bahamas. J. Sediment. Petrol. 56, 422—428.

Thompson, W.G., Goldstein, S.L., 2005. Open-system coral ages reveal persistent suborbital sea-level cycles. Science 308, 401—404.

Thompson, W.G., Spiegelman, M.W., Goldstein, S.L., Speed, R.C., 2003. An open-system model for U-series age determinations of fossil corals. Earth Planet Sci. Lett. 210, 365—381.

Thompson, W.G., Curran, H.A., Wilson, M.A., White, B., 2011. Sea-level oscillations during the last interglacial highstand recorded by Bahamas corals. Nat. Geosci. 4, 684—687.

Thurber, D.L., 1962. Anomalous U^{234}/U^{238} in nature. J. Geophys. Res. 67, 4518—4520.

Vacher, H.L., Hearty, P., 1989. History of Stage 5 sea level in Bermuda: review with new evidence of a brief rise to present sea level during Substage 5a. Quat. Sci. Rev. 8, 159—168.

Vacher, H.L., Rowe, M.P., 1997. Geology and hydrogeology of Bermuda. In: Vacher, H.L., Quinn, T.M. (Eds.), Geology and Hydrology of Carbonate Islands. Developments in Sedimentology, vol. 54. Elsevier, Amsterdam, pp. 35—90.

Vacher, H.L., Rowe, M., Garrett, P., 1989. The geological map of Bermuda, scale 1: 25,000. Hamilton, Bermuda: Public Works Department.

Vacher, H.L., Hearty, P.J., Rowe, M.P., 1995. Stratigraphy of Bermuda: nomenclature, concepts, and status of multiple systems of classification. Geol. Soc. Am. Spec. Pap. 300, 271—294.

Veeh, H.H., 1966. Th^{230}/U^{238} and U^{234}/U^{238} ages of Pleistocene high sea level stand. J. Geophys. Res. 71, 3379—3386.

Vogt, P.R., Jung, W.-Y., 2007. Origin of the Bermuda volcanoes and the Bermuda Rise: history, observations, models, and puzzles. Geol. Soc. Am. Spec. Pap. 430, 553—591.

Wainer, K.A.I., Rowe, M.P., Thomas, A.L., Mason, A.J., Williams, B., Tamisiea, M.E., Williams, F.H., Düsterhus, A., Henderson, G.M., 2017. Speleothem evidence for MIS 5c and 5a sea level above modern level at Bermuda. Earth Planet Sci. Lett. 457, 325—334.

Wehmiller, J.F., Simmons, K.R., Cheng, H., Edwards, R.L., Martin-McNaughton, J., York, L.L., Krantz, D.E., Shen, C.-C., 2004. Uranium-series coral ages from the U.S Atlantic Coastal Plain–the "80 ka problem" revisited. Quat. Int. 120, 3—14.

Weidick, A., 1995. Satellite image atlas of glaciers of the world. Greenland. U.S. Geol. Surv. Prof. Pap. 1386—C.

White, B., Curran, H.A., Wilson, M.A., 1998. Bahamian coral reefs yield evidence of a brief sea-level lowstand during the last interglacial. Carbonates and Evaporites 13, 10—22.

Wilson, M.A., Curran, H.A., White, B., 1998. Paleontological evidence of a brief global sea-level event during the last interglacial. Lethaia 31, 241—250.